

DETERMINING THE ROLE OF ATP6V0E1 OF THE VACUOLAR-
ATPASE IN REGULATING NEUROBLASTOMA CELL SURVIVAL
AND DIFFERENTIATION

By

Geraldo Medrano, B.A.

A thesis submitted to the Graduate Council of
Texas State University in partial fulfillment
of the requirements for the degree of
Master of Science
with a major in Biochemistry
May 2018

Committee Members:

Liqin Du, Chair

Tania Betancourt

L. Kevin Lewis

COPYRIGHT

By

Geraldo Medrano

2018

FAIR USE AND AUTHOR'S PERMISSION STATEMENT

Fair Use

This work is protected by the Copyright Laws of the United States (Public Law 94-553, section 107). Consistent with fair use as defined in the Copyright Laws, brief quotations from this material are allowed with proper acknowledgement. Use of this material for financial gain without the author's express written permission is not allowed.

Duplication Permission

As the copyright holder of this work I, Geraldo Medrano, refuse permission to copy in excess of the "Fair Use" exemption without my written permission.

ACKNOWLEDGEMENTS

To both of my amazing parents, Olivia and Jesus Medrano. For allowing me to discover and pursue my passions while supporting the many paths I have chosen. To my good friend Eliseo Salas who has been a mentor and friend. One cannot forget Nestor and Kimber, the two friends who have been there for me through thick and thin. The great teamwork that has seen us through the darkest of times in our grad school careers. Lastly, to Johanna Villarreal who has been a huge support throughout the years and continues to inspire the best in me and will continue to.

A big thank you to Dr. Liqin Du for providing me the opportunity to develop as a scientist through her mentorship. I appreciated every criticism and advice. I hope that through my actions and work I was able to show my gratefulness for your mentorship. Thank you to both Dr. Kevin Lewis and Dr. Tania Betancourt for all your support.

TABLE OF CONTENTS

	Page
ACKNOWLEDGEMENTS.....	iv
LIST OF TABLES.....	vii
LIST OF FIGURES.....	viii
ABSTRACT.....	ix
CHAPTER	
I. INTRODUCTION.....	1
1.1 Neuroblastoma Tumorigenesis.....	1
1.2 Differentiation Therapy.....	2
1.3 miRNAs.....	4
1.3.1 miRNAs in Cancer.....	7
1.4 The Five Classes of ATPase Enzymes.....	9
1.4.1 The Critical Role of V-ATPase in Diverse Cellular Processes.....	10
1.4.2 V-ATPase Inhibitors.....	12
1.4.3 Mechanisms of Cell Death by V-ATPase Subunit Knockdown.....	13
1.4.4 Shared Subunits between ATPases.....	14
1.4.5 The Role of V-ATPase in Neurotransmitter Release.....	15
1.4.6 Regulation of the V-ATPase.....	15
1.4.7 The Role of the V-ATPase in Endocytosis and Exocytosis.....	16
1.4.8 The Role of the e Subunit in V-ATPase Function.....	17
1.4.9 Pathogenesis and Diseases as a Result of V-ATPase Malfunction.....	18
1.4.10 The Role of the V-ATPase in Cancer and the Underlying Mechanisms.....	18
II. MATERIALS AND METHODS.....	23
2.1 Materials and Reagents.....	23

2.2 Software and Equipment	25
2.3 Cell Culture	25
2.4 Transfections	26
2.4.1 Reverse Transfection of Neurite Outgrowth assay	26
2.4.2 Reverse Transfection of Colony Formation Assay	27
2.4.3 Forward Transfection for Western Blot	28
2.5 Neurite Outgrowth Analysis.....	28
2.6 MTT Analysis.....	29
2.7 Western Blot.....	29
2.7.1 Cell Lysate Collection and BCA Assay	29
2.7.2 SDS-PAGE	30
2.7.3 Transfer.....	31
2.7.4 Blotting.....	31
2.7.5 Re-Blotting	32
2.7.6 Western Blot Quantification	32
2.8 Statistical Analysis.....	32
2.8.1 Neurite Outgrowth Assay	32
2.8.2 MTT Assay	33
2.8.3 Colony Formation Assay	33
2.9 Neuroblastoma cell lines	34
III. RESULTS	35
3.1 Validation of ATP6V0E1 Knockdown.....	34
3.2 ATP6V0E1 Knockdown Does Not Induce Neuroblastoma Cell Differentiation.....	36
3.3 Knockdown of ATP6V0E1 Expression Reduces Cell Viability.....	39
3.4 Knockdown of ATP6V01 Reduces Cell Proliferation	43
IV. DISCUSSION AND CONCLUSIONS	46
REFERENCES	50

LIST OF TABLES

Table	Page
1. Genes down-regulated by miR-506-3p.....	9
2. The materials and reagent used in the experiments are listed.....	23
3. The software used for experiments and analysis are listed.....	25

LIST OF FIGURES

Figure	Page
1. Neural crest precursor pathway in normal and neuroblastoma cells.....	2
2. The interaction between micro-RNA and mRNA.....	5
3. mRNA modes of translation inhibition.....	6
4. The structure and mechanism of the multi-subunit V-ATPase.....	11
5. The ribonucleotide sequences of the treatments used	35
6. Expression changes of ATP6V0E1 determined by qRT-PCR.....	36
7. Neurite outgrowth assay on BE(2)-C cells to detect morphological neural differentiation.....	37
8. Detection of neural differentiation biomarkers in BE(2)-C cells.....	38
9. Neurite outgrowth assay on Kelly cells to detect morphological neural differentiation.....	39
10. The effect of knockdown of ATP6V0E1 on BE(2)-C cell viability.....	40
11. The effect of knockdown of ATP6V0E1 on Kelly cell viability	41
12. The effect of ATP6V0E1 knockdown on SK-N-F1 cell viability.....	42
13. The effect of ATP6V0E1 knockdown on HTB-11 cell viability.....	43
14. The effect of ATP6V0E1 knockdown on BE(2)-C cell colony formation.....	44
15. The effect of ATP6V0E1 knockdown on Kelly cell colony formation.....	45
16. The effects mediated by miR-506-3p	47

ABSTRACT

Neuroblastoma is one of the leading causes of cancer-related childhood deaths. Neuroblastoma arises from the developing sympathetic nervous system where neural crest cells fail to complete the differentiation process. The failure in the differentiation process stimulated the investigation into differentiation-inducing agents capable of activating endogenous differentiation pathways. A high-throughput morphological screen was performed using a library of microRNA mimics to test if microRNA treatment was sufficient to induce neural cell differentiation. The screen identified microRNA 506-3p (miRNA-506) to be a potent tumor suppressor and neuroblastoma cell differentiation inducer.

A gene expression array of neuroblastoma cells treated with miR-506 determined that the gene ATP6V0E1 is directly targeted by miRNA-506 and was the most differentially modulated gene from the list, suggesting it plays a role in mediating the function of miRNA-506 in neuroblastoma cells. The objective of this work was to investigate whether ATP6V0E1 plays a role in regulating neuroblastoma cell survival and differentiation. We observed that by using siRNAs to knock down the expression of the e subunit we were able to reduce neuroblastoma proliferation and cell viability. Knockdown of the e subunit was not sufficient to induce neural cell differentiation.

These results suggest that the e subunit is essential for neuroblastoma cell survival and does not play a role in the neural cell differentiation process. The e subunit has been

shown to be essential for normal V-ATPase function. This evidence suggest that by knocking down the e subunit, V-ATPase efficiency is reduced and the neuroblastoma cells are not able to survive under these conditions.

I. INTRODUCTION

1.1 Neuroblastoma Tumorigenesis

Neuroblastoma is the most common extracranial pediatric solid tumor, accounting for about 15% of pediatric cancer related deaths.¹ Patient age is a robust prognostic in determining patient survival probability. Patients older than 18 months are at more risk of poor outcome than those less than 18 months.²⁻³ Neuroblastoma patients diagnosed at a young age typically don't live past 10 years of age. The high mortality rate of neuroblastoma-affected patients can be attributed to its biological heterogeneity, which renders many multimodal therapeutic strategies ineffective.⁴

Neuroblastoma manifests from the developing sympathetic nervous system, where neural crest cells that typically mature into either sympathetic ganglion cells or adrenal cells fail to complete the differentiation process (**Figure 1**).⁵ Neural crest progenitors experience various extrinsic signals that influence their migration and specification into cells they are destined to become.⁶ Neural crest cells that do not respond to differentiation inducing extrinsic signaling typically undergo apoptosis, but, if cell suicide is evaded, the cell maintains its stem cell state and as a result may develop into a malignant tumor.⁷ Neuroblastoma tumors can form anywhere along the sympathetic nervous system. Sixty-five percent of neuroblastoma tumors are found in the abdomen with the adrenal medulla being a common site for manifestation. Other sites where neuroblastoma can manifest are the neck, chest, and pelvis.⁸ Neuroblastoma's broad spectrum of clinical behaviors and symptoms are directly linked to the primary and metastatic sites of disease. For example, tumors in the abdomen or pelvis lead to

symptoms such as belly pain, lymph and blood vessel blockage, or weight loss.

Metastasis can lead to neuroblastoma spreading to the bones.

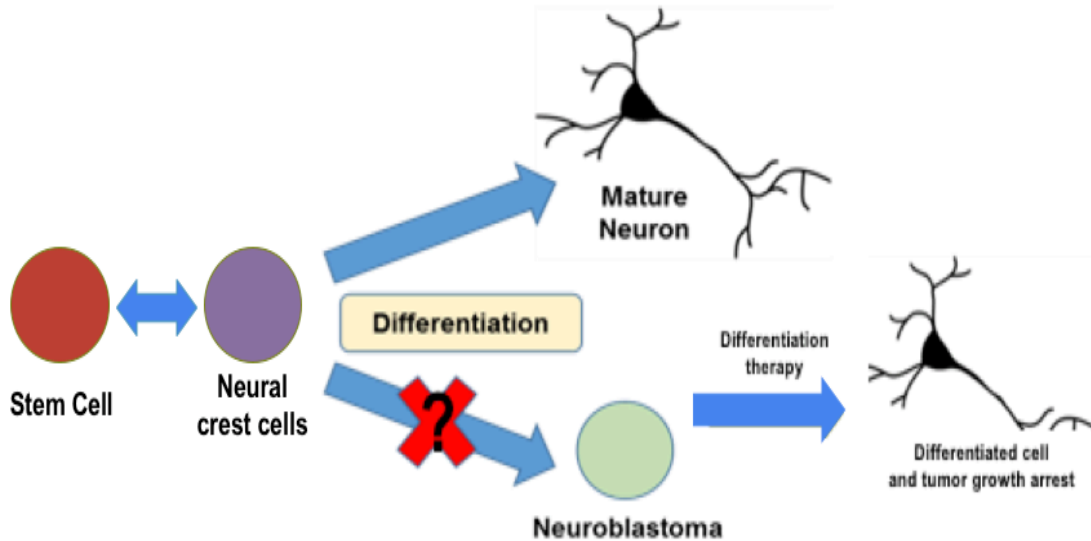


Figure 1. Neural crest precursor pathway in normal and neuroblastoma cells. Stem cells specialize into pluripotent neural crest cells. The neural crest cells specialize into neuroblasts that are thought to be the cells of origin for neuroblastoma. Neural crest precursor cells normally differentiate into mature neurons as depicted by the top half of the diagram. However, neural crest cells that bypass the differentiation process maintain their proliferative ability, which may give rise to malignant cells. Differentiation agents induce the neuroblastoma cells to activate the differentiation pathway, resulting in the cells taking on a more mature stance, inhibiting cancer growth.

1.2 Differentiation Therapy

Traditional treatments for neuroblastoma tumor eradication include surgery, chemotherapy, and radiotherapy. Each treatment is tailored depending on patients age and disease state. Low to medium risk patients showed an overall excellent survival rate. However, high risk patients require a more intense course of action which only leads to an incremental improvement with only 40% of high-risk patients surviving.⁹

Conventional treatments generally involve killing the tumor cells while in the process

potentially damaging or killing normal cells. Few high-risk patients become long term survivors with conventional therapeutics, indicating the requirement for the investigation into different therapeutic strategies. Poorly differentiated or undifferentiated histology is an independent indicator of poor prognosis.¹⁰ The aberration of neuroblastoma's differentiation pathways stimulated investigations into the mechanisms involved, paving the way for the alternative method of treatment termed differentiation therapy.

Differentiation therapy is an approach that aims to reactivate the endogenous differentiation programs of cancer cells (**Figure 1**) by targeting biological molecules that play a role in neuroblastoma cell differentiation.¹¹ Several signaling molecules and agents have been used to induce differentiation and show clinical benefits. Examples of these are: angiogenesis inhibitors, tyrosine kinase inhibitors, demethylating agents, histone deacetylase inhibitors, heat shock protein 90 inhibitors, and retinoids.⁸ Exogenous influence on the maturation of the neuroblastoma cells has shown to result in the reduction or loss of the cancerous phenotype and leads to tumor growth arrest by inhibiting cellular proliferation.¹² This mode of action is very attractive, but a deeper understanding of the mechanisms involved in the biology of the normal differentiation pathways is needed.

Differentiation agents are thought to be less cytotoxic than conventional cancer treatments. Currently, the differentiation agent 13-cis-retinoic acid (RA) is the standard of care for post-remission maintenance therapy in high risk neuroblastoma.¹³⁻¹⁴ RA induces morphological and functional changes that mimic the normal differentiation of neural crest precursors into mature neurons. Clinical trials where patients were treated with RA as a maintenance therapy after undergoing myeloblative therapy showed

improved outcome leading to RA becoming a standard in neuroblastoma treatment.¹⁵ RA is a derivative from the bioactive metabolite of vitamin A, all-trans retinoic acid (ATRA). ATRA and RA have both been shown to regulate mechanisms involved in cell proliferation, differentiation, and apoptosis in normal and cancer cells.¹⁶⁻¹⁷ Cell lines exposed to either RA or ATRA exhibit a reduction in proliferation, expression of the N-Myc oncogene, and exhibit induced neuronal differentiation. However, there are still many high-risk neuroblastoma patients whose tumors do not respond to RA. Alternate strategies is the next logical step in neuroblastoma treatment.

Various differentiation agents have been investigated and characterized. For example, upregulation of microRNA-449a via a microRNA-449a mimic was shown to induce differentiation in neuroblastoma and other cell lines.¹⁸ Three target genes, MFAP4, PKP4, and TSEN15, were found to be involved in the cell differentiation process. Two of the target genes, CDK6 and LEF1, were shown to play a critical role in cell cycle arrest. In addition, the mRNA expression levels of these targets in neuroblastoma tumor specimens are correlated to patient survival, with high expression levels correlated with poor patient survival. Further studies into the mechanisms involved in regulating the neuroblastoma cell differentiation process via molecular compounds can lead to the development of differentiation agents targeting genes that play important roles in both neuroblastoma differentiation and growth.

1.3 miRNAs

MicroRNAs (miRNAs) are endogenous non-coding ribonucleotide oligomers (~20-30 nucleotides long). Typically, one miRNA regulates a set of mRNAs rather than only one mRNA. miRNA-mediated post-transcriptional processes play an important role

in regulating gene expression and various biological functions such as cell proliferation, apoptosis, differentiation, and other cellular processes.¹⁹ The post-transcriptional process involves a complex where the miRNA acts as a guide and the associated argonaute proteins act as the effectors. miRNA target binding is typically achieved via a sequence-specific base-pairing at the 3' UTR or 5' UTR of the mRNA target (**Figure 2**).²⁰⁻²¹ The seed sequence that is hybridized is conserved and recognized by the miRNA. The 3' UTR binding site is a key determinant for target specificity within miRNA families. Currently, there are four types of recognized seed sequences: 6-mer, two types of 7-mer, and an 8-mer with complementarity increasing in that order. Complementarity does not always result in suppression of a target. There are other parameters that must be met in order for miRNA binding to result in repression of its target. In addition to the 3' seed sequence, the downstream 3' binding sequence (nucleotides 12-17) can compensate for any mismatches in between the target mRNA and miRNA.

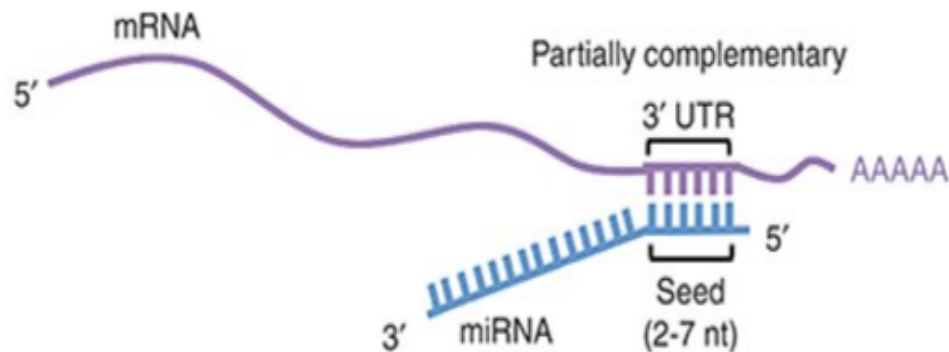


Figure 2: The interaction between micro-RNA and mRNA. MicroRNAs bind to the 3'-untranslated region (UTR) or 5' UTR of a targeted mRNA by complementary base pairing.

The miRNAs get incorporated into the RNA-induced silencing complex (RISC), where it guides the complex to the target mRNA and the endonuclease of the RISC complex cleaves the mRNA. The degree of complementarity between the miRNA and its target mRNA determines the pathway taken to silence translation. The two pathways of post-transcriptional repression are mRNA cleavage or translational repression as seen in **Figure 3**. When there is sufficient complimentary binding the miRNA target gets cleaved. After cleavage of the target site, the RISC complex stays intact and is capable of continuing its effects on other mRNA targets. If there is not sufficient mRNA complementarity, translational repression is the route taken.

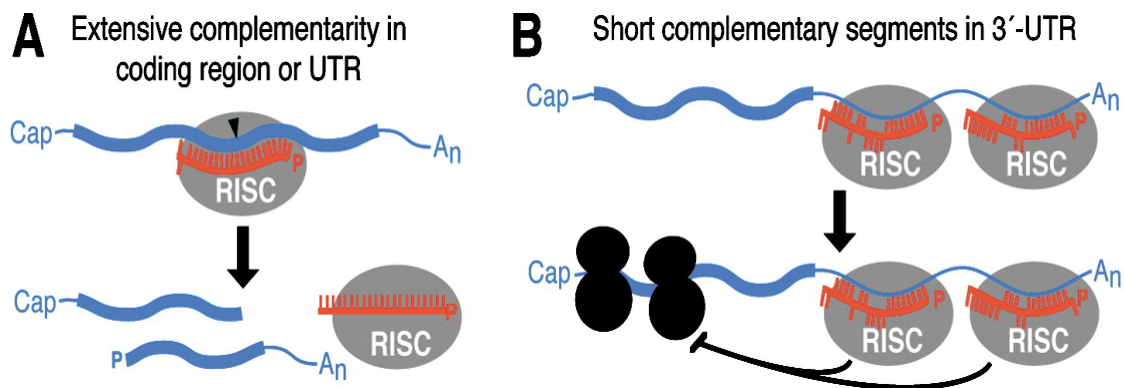


Figure 3. miRNA modes of translation inhibition. **A.** The RISC complex uses the miRNA as a guide to bind to an mRNA target. Once bound, the endonuclease portion is able to degrade the mRNA target. **B.** The RISK complex is capable of binding the mRNA target and inhibiting translation by blocking the ribosomes from attaching.

Humans have more than 60% of their protein coding genes containing a conserved miRNA binding site.²² This fact with the knowledge that there are numerous non-conserved miRNA binding sites indicates that there must be a high degree of regulation of miRNA biogenesis and function.

miRNA mimics have been developed as a tool to mimic the endogenous function of a specific miRNA. The miRNA mimics are partially double-stranded RNAs that get utilized in the same manner as the endogenously derived miRNA. These molecules have been utilized as tumor suppressors to inhibit cancer growth.¹¹

1.3.1 miRNAs in Cancer

Aberrant expression patterns of miRNA are associated with cancer pathogenesis.²³⁻²⁵ In B-cell chronic lymphocytic leukemia, miR-15 and miR-16 were associated with tumor pathogenesis when they were shown to be located in a deleted region of chromosome 13q14. In addition, miR-15 and miR-16 expression levels were either down-regulated or not detected in almost 70% of malignant B-cells.²⁶ These results suggest that the dysregulation of miRNA expression is involved in carcinogenesis. The effects of a differentiation agent, all-trans retinoic acid (ATRA), on miRNA regulation was investigated in human acute promyelocytic leukemia. Morphological changes indicative of induced granulocytic differentiation were observed in the acute promyelocyte cells.²⁷ ATRA upregulated the expression of miRNAs involved in tumor suppression. The upregulation of the miRNAs was validated by the downregulation of their target mRNA and proteins, indicating that dysregulation of miRNAs may underlie cancer pathology. Let-7 is a conserved miRNA found to be involved in regulating the developmental process in bilaterian animals²⁸ The Let-7 studies stimulated the investigation of both its role and that of other miRNAs in cancer development. MiRNA expression abnormality was investigated in lung cancer tissues which provided evidence of extensive alterations in miRNA and miRNA-precursor expression.²⁹⁻³⁰ Overall, these investigations suggest that miRNA dysregulation plays a role in cancer development.

It's clear that the transition from the pluripotent, self-renewing state of the neural crest cell to more specialized neuroblast state is accompanied by a shift in the miRNA populations present in the cell. A high-content morphological screen was used to identify novel neuroblastoma differentiation-inducing miRNAs. The screen identified miRNA-506-3p (miR-506) as a potent neuroblastoma differentiation inducer and growth inhibitor.¹¹ A microarray was generated using the predicted targets of the miR-506 identified via Ingenuity Pathway Analysis (IPA) to determine the extent of influence the miRNA had on each target. Table 1 shows a portion of the genes that were differentially expressed in miR-506-treated cells.

The genes, CDK4 and STAT3 were shown to be down-regulated by miRNA-506 treatment. This was validated by the down-regulation of CDK4 and STAT3 protein expression levels due to overexpression via transfection of miR-506 mimic in neuroblastoma cells. Suppression of both CDK4 and STAT3 expression individually and in combination induced neurite outgrowth in neuroblastoma cells, indicating their role in the differentiation inducing function of miR-506. ATP6V0E1 gene is the top differentially modulated gene. ATP6V0E1 encodes a subunit that is known to be part of the V-ATPase complex. Due to the fact that it was the gene affected the most by miR-506-3p, we decided to characterize its role in mediating the effects of miR-506-3p in neuroblastoma cells.

Table 1: Genes down-regulated by miR-506-3p: this table provides a quantitative list of the genes that are down-regulated by 2.5 fold in BE(2)-C cells by miR-506-3p, and the oligo negative control. (* = function/regulation not yet defined)

TargetID	Negative control oligo (25nM)	miR-506-3p mimic (25nM)	Ratio	Chrom. Location	Function/Regulation	Target miR-506-3p
ATP6V0E1	2743.8	666	0.24	5q35.2a	ATPase - active transport (H ⁺)	yes
ITGB1	1331.9	421.6	0.32	10p11.22b	cell adhesion, embryogenesis	yes
LASS2	1088.4	378.3	0.35	1q21.2d	cell growth regulation	yes
C11ORF82	1156.4	412.2	0.36	11q14.1d	DNA repair, cell survival	no
ANXA5	1438.9	516.8	0.36	4q27c	growth & differentiation	yes
CDCA7	3322.9	1202.5	0.36	2q31.1e	transcriptional regulator, apoptosis	yes
LAMC1	2650.7	983	0.37	1q25.3d	cell differentiation, neurite outgrowth	yes
C11ORF75	1963.3	735	0.37	11q21a	membrane protein*	yes
SYPL1	1395.2	524.5	0.38	7q22.2c	transporter activity	yes
CMTM7	3009.8	1141.8	0.38	3p22.3c	cytokine activity	yes
VAMP3	1047.4	398.5	0.38	1p36.23b	membrane protein, binding	yes
FAM57A	601.2	230.6	0.38	17p13.3f	acetyl-transferase activity	no
CYB5A	1693.7	652.7	0.39	18q22.3c	Fe-reductase	yes
CDK4	5589.4	2195.5	0.39	12q14.1a	G1 phase progression by Rb	yes
CDKN1A	838.5	333.2	0.40	6p21.31a	G1 phase progression – CDK inhibitor	no
MYH9	1402.5	560	0.40	22q12.3d	motility & cell morphology	yes
MCM4	3440.5	1375.4	0.40	8q11.21b	genome replication – pre-rep. complex	no

1.4 The Five Classes of ATPase Enzymes

ATPases are a class of enzymes that couple the hydrolysis/synthesis of ATP to the translocation of solutes across membranes. There are several types of ATPases that vary in their location, function, and in the solutes they translocate across the membrane. F1-F0 synthase (F-ATPases) are found in the membranes of mitochondria, chloroplasts and bacterial plasma membranes. These enzymes couple the synthesis of ATP to proton transport across the membrane.³¹ Archaeal ATPases (A-ATPases) have been found in archaea exclusively. A-ATPases are structurally similar to V-ATPases, but have a function similar to F-ATPase. A-ATPases utilize a proton gradient for the synthesis of ATP.³² A-ATPases have been postulated to have arisen as an adaptation to the different cellular needs and extreme environmental conditions faced by the archaeal species.

P-ATPases are found in bacteria, fungi, and in a number of eukaryotic plasma and organelle membranes. There are various subclasses of P-ATPases that function in coupling ATP hydrolysis to cation uptake and/or efflux.³³⁻³⁴ Cations identified to be involved in the translocation process are: H^+ , Na^+ , K^+ , Mg^{2+} , Ca^{2+} , Ag^{2+} , Zn^{2+} , Co^{2+} , Pb^{2+} , Ni^{2+} , Cd^{2+} , Cu^+ and Cu^{2+} . Extracellular membrane-bound cell surface enzymes (E-ATPases) have a broad range of substrate specificities, hydrolyzing other nucleotide triphosphates besides ATP³⁵. The Vacuolar ATPase (V-ATPase) couples ATP hydrolysis to the translocation of protons across the membrane. More detail about the enzymatic activity of V-ATPase will be explained below. All five general classes of ATPases contain similar subunits, where certain parts were fine-tuned through the evolutionary process to adapt to work under particular physiological conditions and environmental pressures.³⁶

1.4.1 The Critical Role of V-ATPase in Diverse Cellular Processes

The Vacuolar (H^+)-ATPase (V-ATPase) is a highly conserved multi-subunit enzyme composed of an integral membrane sector (V_0) and a peripheral catalytic sector (V_1) (**Figure 4**). The mammalian V-ATPase is composed of 13 subunits. The V_1 sector is comprised by subunits A, B, C, D, E, F, G and H. The V_0 domain is composed of a, c, c', d, and e subunits. Many of the subunits have various isoforms and some of these isoforms have been found to be tissue-specific. The V-ATPase couples the energy from ATP hydrolysis to transport protons across the intracellular and in some specialized cells, plasma membranes. The V-ATPase complex was first discovered in the vacuolar membranes of yeast which may be an indication that the enzyme is required for basic cell

physiology, maintaining housekeeping functions.³⁷ It is now known that V-ATPase is present in both uni- and multicellular organisms, including plants and animals.

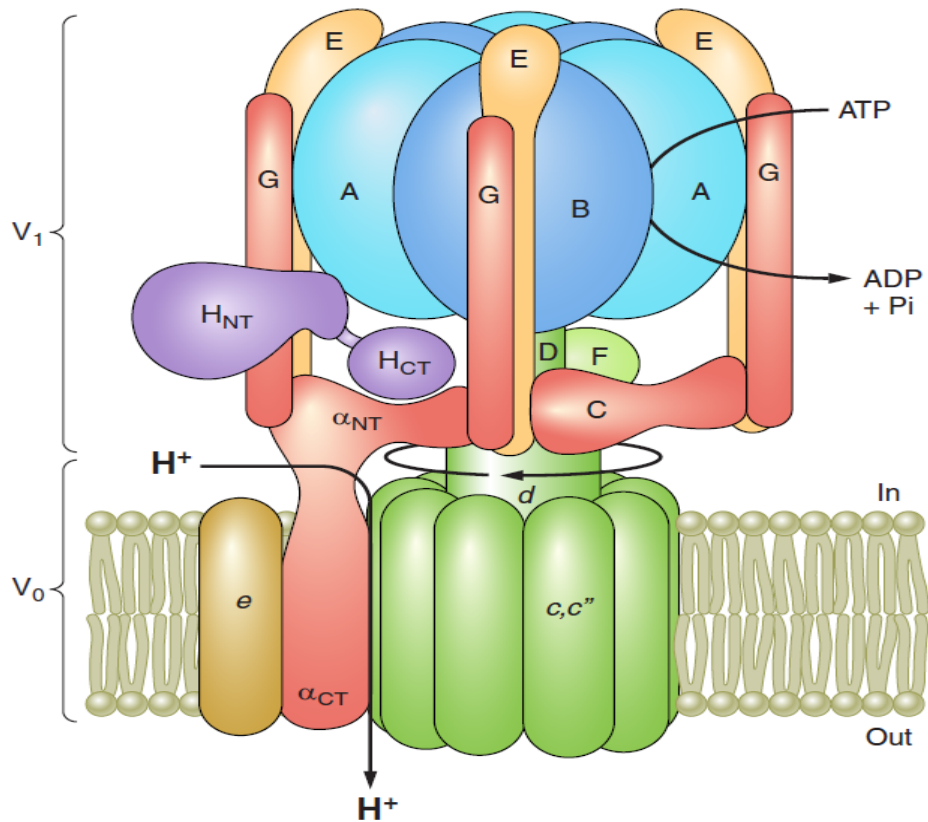


Figure 4. The structure and mechanism of the multi-subunit V-ATPase. The V-ATPase is composed of a peripheral V₁ domain that is responsible for ATP hydrolysis and a membrane-bound V₀ domain responsible for translocating protons.³⁸

The enzyme complex is distributed across various intracellular membranes such as the lysosomes, endosomes, secretory vesicles, and for specialized cell types, the plasma membrane.³⁹ The acidic environment generated by the V-ATPase is required for a variety of cellular processes and disruption results in the aberration of multiple biological processes. In the lysosome, the V-ATPase generates an acidic environment for optimal

proteolytic activity for enzymes residing in the lysosome.⁴⁰ In addition to providing an ideal pH for enzyme activation, the acidic pH influences conformational distortions in the proteins located inside, making protein degradation easier for the proteolytic enzymes. The pH gradient generated across lysosomal membranes is used to drive the coupled transport of small molecules out of the membrane, such as amino acids following protein degradation.⁴¹ Interestingly, the V-ATPase has also been implicated in amino acid sensing.⁴² The electrochemical gradient established by V-ATPase in neuronal synaptic vesicles is utilized as the driving force for the uptake of the neurotransmitter glutamate.⁴³ Specialized cells contain V-ATPase in their plasma membrane. Acid-base homeostasis in the kidney is regulated by V-ATPase in the plasma membrane of intercalated cells.⁴⁴ In bone, osteoclasts generate an acidic microenvironment that is essential for bone reabsorption.⁴⁵ These findings indicate that V-ATPase supports critical physiological processes and fundamental cellular function through its proton translocating activity.

1.4.2 V-ATPase Inhibitors

Targeting the different molecular subunits provides insight into the functional importance of each component in the V-ATPase complex. The V-ATPase is considered an attractive target in chemotherapy due to the increasing evidence of its role in cancer. Various V-ATPase inhibitors have been discovered and their mechanism of actions are being investigated.⁴⁶ The plecomacrolides, Bafilomycin and Concanamycin, are two of the first V-ATPase inhibitors discovered and have been extensively researched since. Both plecomacrolides inhibit the function of the V-ATPase by interacting with the c subunit in the V_0 domain which results in the inhibition of proton translocation.⁴⁷ In

addition to the c subunit, Bafilomycin has been shown also interact with the a subunit of the V_0 domain.⁴⁸ The main issue with the plecomacrolides is their specificity for the ATPases. Subunit c is highly conserved amongst the various ATPases and when cells are treated with plecomacrolides, there is inhibition of the other ATPases in the cell.

The inhibitor, Archazolid, was recently discovered in a screen for novel antibiotics produced by mycobacteria. Exposure to Archazolid induced the formation of vacuoles in the endoplasmic reticulum and the prevention of lysosomal acidification indicating morphological effects comparable to those of concanamycin and bafilomyacin.⁴⁹ Archazolid prevented the binding of both bafilomyacin and concanamycin suggesting that the V_0 subunit c is the target binding site.⁵⁰

The main issue with the traditional V-ATPase inhibitors is their lack of specificity which would be highly toxic for all cells and not fit for medicinal use. These inhibitors bind to the subunits in the V_0 region, with most binding to the highly conserved c subunit.⁴⁷

1.4.3 Mechanisms of Cell Death by V-ATPase Subunit Knockdown

Evidence is increasing that the V-ATPase plays a role in cancer based on observations of increased expression and activity of the V-ATPase in the plasma membrane of tumor cells.⁵¹ In response, several V-ATPase inhibitors have been developed and investigated to elucidate their effects on cancer cells. Various studies suggest that the result of targeting the V-ATPase is induced apoptosis. Colon cancer cells treated with the V-ATPase inhibitor Bafilomycin A_1 were observed to undergo apoptosis enhanced by the inhibition of macroautophagy which is considered a prosurvival process.⁵² Gastric cancer cells treated with Bafilomyacin A_1 results in the induction of

apoptosis. This is supported by the increased expression of the activated form of caspase-3 via a cytochrome-independent manner.⁵³ Apoptosis was induced in both breast and pancreatic cancer cell types after treatment with the V-ATPase inhibitor Archazolid. Archazolid induced apoptosis via caspase activation and did not impair the mitochondria like Bafilomycin and concanamycin, which may affect P-ATPases as secondary targets.⁵⁴ The pesticide pea albumin 1 subunit b (PA1B) targets the a and e subunits of the V_0 portion of the V-ATPase resulting the inhibition of proton translocation.⁵⁵ The ingestion of PA1B results in apoptosis and ultimately insect death. Increased expression levels of activated caspase-3 is observed, but whether caspase-3 was activated via a mitochondrial or membrane pathway was yet to be determined. A non-apoptotic death is observed in yeast where the V-ATPase facilitated the release of toxic materials into the cytoplasm by permeabilizing the vacuolar membrane.⁵⁶ Necrotic cell death facilitated by the cytoplasmic acidification via V-ATPase is observed in *C. elegans*. Acidification was found to be a factor required for the endoplasmic reticulum to release its calcium stores, resulting in elevated levels of cytoplasmic calcium. Increased calcium resulted in the activation of a calpain-induced necrotic cell death.⁵⁷

1.4.4 Shared Subunits Between ATPases

The V-ATPase belongs to the class of pumps that includes the structurally similar F_0 - F_1 -ATP synthase (F-ATPase). The F-ATPase functions in the synthesis of ATP in chloroplasts, mitochondria, and bacteria.⁵⁸ This class is distinguished from the other ATPases because they are composed of two multi-subunit sectors: a transmembrane sector and a detachable catalytic sector. The V- and F-ATPases are thought to originate from a common ancestor due to their sequence similarity. Interestingly enough, the V-

ATPase has greater sequence similarity to the subunits of A-ATPases than F-ATPases.⁵⁹

The subunits in V1 are designated A-G in order of decreasing mass. In yeast, the inactivation of any subunit, with the exception of Vph1p, results in V-ATPase malfunction. The consequences are not lethal, but include sensitivity to high levels of calcium and a dysfunctional vacuole.⁶⁰⁻⁶¹

1.4.5 The Role of V-ATPase In Neurotransmitter Release

Neurotransmitters are released from the presynaptic terminal into the synaptic cleft via fusion of synaptic vesicles with the plasma membrane. V-ATPases were found to be present in neurotransmitter storage organelles and synaptic vesicles suggesting an important role in secretory function.⁶² V-ATPase plays a critical role in both neurotransmitter uptake and exocytosis. V-ATPase contributes to vesicle loading with neurotransmitters by providing a synaptic vesicle membrane potential. Neurotransmitter transporters utilize the synaptic membrane potential to load glutamate or proton co-transport to translocate GABA, acetylcholine, and monoamines.^{43, 63-64} Vesicle release requires complexing between SNARE (“soluble NSF attachment receptor”) proteins, one in the plasma membrane and the other in the vesicle membrane. V_0 has been observed to act as a regulatory mechanism by binding to the Q-SNARE protein, inhibiting it from complexing with R-SNARE. When V_0 binds to Q-SNARE, vesicle fusion is prevented, suggesting a role for V_0 in the membrane fusion process.⁶⁵

1.4.6 Regulation of the V-ATPase

The assembly of the V-ATPase complex is fascinating because it is composed of both integral membrane proteins and peripheral proteins. The V_0 domain is synthesized and assembled in the endoplasmic reticulum and transported to the Golgi. In the Golgi,

the V_0 domain will receive an assembled V_1 domain that was assembled in the cytosol.⁵¹ The V_1 and V_0 sectors do not show H^+ proton translocating activity when not associated as a holoenzyme.⁶⁶ V-ATPases containing unique isoforms of particular subunits are only found in certain cell types or even particular organelles. This means that cellular targeting must be very precise to function properly. Misplacement of a V-ATPase alters the local pH of where it is placed. In addition, it's been shown that V-ATPase assembly is dynamic and is influenced by extracellular events.

Currently, there are two different views of V-ATPase assembly that are generally agreed upon. The Concerted pathway involves the V_1 and V_0 subunits interacting and building upon each other. The Independent pathway involves the two sectors assembling independent of each other, but then coming together once the domains are assembled.⁶⁷

1.4.7 The Role of the V-ATPase in Endocytosis and Exocytosis.

Endocytosis and exocytosis are fundamental processes used for the transportation of various molecules across cell membranes. The V-ATPase plays a key role in internalizing cellular receptors at the plasma membrane.⁶⁸ After the receptor's corresponding ligands binds, the receptor/ligand complex initiates signaling and is then retrieved from the plasma membrane via the trafficking endosomal/lysosomal pathway. This pathway can go two routes: i) the receptor/ligand pathway involves delivery via clathrin-coated vesicles to early endosomes, multivesicular bodies, late endosomes and then to lysosomes for acidification-dependent degradation. ii) the receptor/ligand complex undergoes a V-ATPase-dependent ligand dissociation process where the acidification of the vesicle causes the ligand to be released. After release, the receptors

are typically recycled and returned back into the plasma membrane via recycling endosomes.

1.4.8 The Role of the e Subunit in V-ATPase Function

The miRNA-506-3p has been shown to target the e subunit of the V-ATPase in neuroblastoma cells. Although the e subunit is not very well characterized, it is postulated to be located in the transmembrane V_0 portion of the V-ATPase and essential for V-ATPase function.⁶⁹⁻⁷¹ Work in yeast has demonstrated that the e subunit is an integral membrane protein that is essential for V_0 subcomplex assembly, where mutation results a nonfunctioning V-ATPase complex.⁷² Localization of the e subunit in the endoplasmic reticulum was observed and its transportation to the vacuole was hindered with the deletion of any of the V_0 subunits. In humans, there are two isoforms of the e subunit that both show tissue-specific expression.⁷³ Knockout of the e subunit orthologue gene in yeast, VMA9, is lethal. Transformation with either the e1 and e2 isoforms was sufficient to restore growth capabilities of e subunit-deficient yeast strains, supporting their structural and functional similarity. Analysis of the two cDNA isoforms showed that the 3' UTR of the e2 subunit is longer than the e1 3' UTR, which may be an indicator of why one isoform was differentially modulated more than the other. Interestingly, in yeast it has been shown that the e subunit is absent from the V-ATPase complex after purification.⁷⁴ However, the e subunit is found in *M. sexta* after purification.⁷⁵ The EM structure derived from *M. sexta* reveals a distinct structure protruding from the base of the V_0 portion when compares to the yeast EM.⁷⁶ In addition, the selective and potent V-ATPase inhibitor Pea albumin toxin 1b (PA1b) was shown to bind to the corresponding location of the e subunit on the EM map.⁷⁷ A genetic screen resulted in the identification

of the e subunit in yeasts. The e subunit was observed to be associated with the V_o portion of the V-ATPase and shown to be essential to V-ATPase function.⁷¹ Knockout mutations of the e subunit in yeasts result in a dysfunctional V-ATPase and required an acidic environment to grow. The reintroduction of e1 was sufficient to restore the ability of the yeast cells to grow at physiological pH.⁷³

1.4.9 Pathogenesis and Disease as a Result of V-ATPase Malfunction

The importance of various subunits has been highlighted by the identification of genetic defects resulting from the absence of specific V-ATPase subunits. The first human disease linked to the V-ATPase complex was the ATP6B1 gene mutation, which encodes the B subunit of the V1 portion of the V-ATPase complex.⁷⁸ Patients with the ATP6B1 mutation experience renal tubular acidosis due to the impaired urinary acidification process, disrupting the critical acid-base homeostasis. This observation indicates the importance of the B subunit in V-ATPase function. Sequencing data from nine patients with autosomal recessive malignant osteoporosis revealed a mutation in the TCIRG1 gene, which encodes a subunit of the V-ATPase.⁷⁹ The same phenotype is experienced when the Atp6i gene, encoding an osteoclast-specific proton pump subunit, is disrupted in mice.⁸⁰

1.4.10 The Role of the V-ATPase in Cancer and the Underlying Mechanisms

One of the hallmarks of cancer is the shift in energy production from oxidative phosphorylation to aerobic glycolysis. NADH is recycled to its oxidized form by the reduction of pyruvate to lactic acid. This reaction results in excess intracellular acidosis due to increased H^+ production per consumed glucose molecule.⁸¹⁻⁸² These protons need to be removed in order to maintain optimal cytosolic pH for cell homeostasis. To enhance

excess proton removal resulting from the high-glycolytic activity of the tumor cell, V-ATPase's expression is typically increased.

The V-ATPase is primarily located within the intracellular membranes of organelles, while in the plasma membrane of only specialized cells such as the kidney vas deference intercalated cells and bone osteoclast cells. Increased expression of V-ATPase in both the plasma and intracellular membranes was observed in human breast cancer cells where they investigated the role of V-ATPase on cytoplasmic pH regulation after exposure to acute acid loads induced by NH_4Cl .⁸³ The levels of V-ATPase expression corresponded to the rate of recovery following acute acid loads, with higher levels corresponding to faster recovery. Inhibition of V-ATPase using bafilomycin decreased the recovery rate. This suggests that the increase in proton pump expression plays a role in cytosolic pH regulation, allowing cells to avoid the cytotoxic effects induced by acidosis. The Ohta research group observed an increase in V-ATPase expression levels in human pancreatic tumor cells compared to normal pancreatic cells.⁸⁴ In this study, immunohistochemistry was used to detect the distribution and localization of V-ATPase in normal and malignant pancreatic cells. 90% of the pancreatic cells displayed increased immunoreactivity compared to normal cells, suggesting V-ATPase may play a specialized role in tumorigenesis. Inhibition of V-ATPase has been shown to result in apoptotic cell death in multiple cancer cell lines. In a study by the Gottlieb lab, neutrophils treated with Bafalomyacin A_1 underwent apoptosis due to intracellular acidification.⁸⁵ Increased expression of the V-ATPase was able to inhibit apoptosis. These findings suggest the primary role of V-ATPase is regulating intracellular acidification, which typically results in apoptosis when dysregulated. The Nikashima

research group showed that the V-ATPase inhibitor, bafilomycin A₁, significantly suppressed the cell growth and induced apoptosis in gastric cancer cells.⁵³ Lysosomal pH had increased, indicating that apoptosis was induced by the activation of caspase-3. The function of V-ATPase is critical in the maintenance of lysosomal pH and suppression of apoptosis induced via lysosomal alkalosis. Intracellular apoptosis was induced in B cell hybridoma cells treated with the V-ATPase inhibitor, Concanamycin A₁.⁸⁶ Cytosol from Concanamycin treated cells had a cytotoxic effect on B cells indicating that the inhibition of V-ATPase may contribute to the induction of the cytotoxic effects. This same research group had previously reported that Concanamycin A₁ induced apoptosis in several eukaryotic cell lines, and that the acidification of intracellular compartments was inhibited when cells were treated with Concanamycin. These studies suggest that V-ATPase plays a key role in mediating cell survival and the induction of apoptosis. Overall, there is clear evidence supporting the important role of V-ATPase in cancer. However, the underlying mechanisms are not fully characterized and warrant further investigation.

Hypothesis and Specific Aims

Microarray analysis of the miR-506-treated cells identified vacuolar (H⁺)-ATPase V₀ subunit e1 (V-ATPase) as a direct target, potentially mediating the tumor suppressive function of differentiation-inducing miRNA miR-506-3p (**Table 1**). V-ATPase has been shown to be aberrantly expressed in malignant cells and even more so in highly metastatic cells. Cell survival in an acidic environment is correlated to the increase in V-ATPase expression as suggested by the induction of apoptosis via V-ATPase inhibitors. Altogether, these findings suggest that the V-ATPase enzyme may play a role in neuroblastoma tumorigenesis. My hypothesis is that V-ATPase plays a role in mediating cell survival and cell differentiation processes. The goal of my project is to determine the role of V-ATPase in modulating neuroblastoma cell survival and differentiation into mature neuronal cells. My specific aims are:

Aim 1: To determine whether V-ATPase regulates neuroblastoma cell survival and proliferation. To accomplish this, neuroblastoma cells were transfected with siRNAs targeting ATP6V0E1 to knockdown the expression of the e subunit. Western blot analysis was used to detect V-ATPase protein expression and ensure protein expression was silenced. Real-Time Quantitative Reverse Transcription PCR (qRT-PCR) assays were used to measure V-ATPase mRNA expression levels. Neuroblastoma cell viability was evaluated using the MTT assay to measure cell metabolic activity. Colony formation assays were used to observe the effects of V-ATPase expression levels on cell proliferation.

Aim 2: To determine whether V-ATPase regulates neuroblastoma cell

differentiation. A neurite outgrowth assay was used to robustly measure *in vitro* morphological changes that are characteristic of differentiated neuroblastoma cells. Western blot analysis was used to detect the expression of markers indicative of a differentiated neuroblastoma cell, such as growth-associated protein (GAP43), Neuron-specific enolase (NSE), and β -Tubulin III. qRT-PCR analysis detected and measured the mRNA expression levels of the neuronal cell differentiation markers.

II. MATERIALS AND METHODS

2.1 Materials and Reagents

Table 2: The materials and reagents used in the experiments are listed:

Materials	Company
Acrylamide/Bis-Acrylamide 29:1 40% solution	Fisher
Albumin Standard	Pierce BCA Assay
Ammonium persulfate	Fisher
Bromophenol Blue	Fisher
Crystal Violet Stain	Fisher
Dharmacon microRNA mimics and control oligos	Fisher
DMEM	Fisher
DMSO	Fisher
DPBS	Fisher
FBS	Atlas Biologicals
Glycerol	Fisher
HCl	Fisher
KCl	Fisher
Lipofectamine RNAiMax	Fisher
Methanol	Fisher
MTT Reagent	Fisher
NaOH 1%	Corning
NaCl	Fisher
Non-Fat Powdered Milk	Boston Bioproducts

Penicillin-Streptomycin	Fisher
Pierce BCA Assay Reagent A	Fisher
Pierce BCA Assay Reagent B	Fisher
PVDF Membranes	Fisher
Rabbit anti-GAP43, anti-NSE, and anti-Beta Tubulin III	Abcam
Rabbit anti-Calnexin and goat anti-rabbit secondary antibody Conjugated with horseradish peroxidase (HRP)	Sigma
Running buffer 1X	National Diagnostics
Spectra multicolor broad range protein ladder	Fisher
SuperSignal West Dura	Fisher
SuperSignal West Pico	Fisher
TEMED	Fisher
Transfer Buffer IX	National Diagnostics
Tris	Fisher
Trypsin	Fisher
Tween 20	Fisher
2-mercaptoethanol	Fisher
All other items were obtained through Fisher	

2.2 Software and Equipment

Table 3: The software used for experimentation and analysis are listed.

Software	Company/Location
Canon CanoScan 9000F MarkII	Aurora, IL, USA
Canon ScanGear Tool Software 64bit windows 7	Bangrak, Bangkok, Thailand
ChemiDocXRS+ System	BioRad, Hercules, CA, USA
Graphpad Prism 7.01	Graphpad Software, La Jolla, CA, USA
Image J	NIH, Bethesda, MD
ImageLab Software Model ChemiDoc XRS+	BioRad, Hercules, CA, USA
NeuroTrack System	Essen Bioscience, Ann Arbor, MI, USA
ZOOM IncuCyte Imaging System	BioTek, Winooski, VT, USA

2.3 Cell Culture

Cell lines were grown and passaged in DMEM supplemented with 10% Fetal Bovine Serum and 5% penicillin streptomycin antibiotic. Cells were passaged every three to five days, depending on how quickly they grew to confluence. Cells used in experimental procedures were only passaged twenty times to reduce the risk of conflicts due to mutation accumulation. To passage the cells, the cell media was suctioned off and discarded. two mL of DPBS (room temperature) was added to wash the cells. DPBS was then suctioned off and two mL of warmed (37°C) trypsin was added and the Petri dish was placed in the 37°C incubator for five minutes. The cells were suctioned up using a pipette and placed in an Eppendorf tube. Fifty µl of full culture media is added to the

Eppendorf tube containing the cells to neutralize the trypsin. The cells were then spun down for three minutes at 3,000 RPM. The supernatant was discarded and full culture media was added to the Eppendorf tube. Using a pipette, the cell clump was broken apart to achieve an even distribution. The cells were then transferred to a 100 mm dish containing warm full culture media.

A hemocytometer was used for cell counting. The four outside square and one middle square were counted to calculate the number of viable cells per milliliter. After counting the cells, we multiplied that value by 10,000 to obtain the number of cells per microliter.

2.4 Transfections

2.4.1 Reverse Transfection of Neurite Outgrowth Assay

Cell counting was performed as mentioned above and the appropriate calculations were done to determine how much cell suspension was needed to have approximately 2,500 cells per well in a 96-well plate. Cells were added to a working cell mixture that had incomplete cell media (DMEM with 10% FBS and no antibiotics) and one μl of the appropriate control siRNA, treatment siRNA or miR-506-3p was added into each well with a concentration of 2.5 nM. Lipofectamine RNAiMax liposomes were prepared in plain media in a separate Eppendorf tube. After a five minute incubation at room temperature, thirty μl of liposome suspension was added to each well. The plate was then vortexed and spun down twice. Following a twenty minute incubation period, 100 μl of cell suspension was added to each well. The plate was then placed in the ZOOM InCuCyte NeuroTrack Imaging System for imaging and monitoring. After twenty-four

hours, seventy μ l of 20% FBS full culture media was added to each well and placed back into the InCuCyte for further imaging.

2.4.2 Reverse Transfection of Colony Formation Assay

After dissociating cells, calculations were done to determine how much cell suspension was needed to plate 2,000 and 4,000 cells per plate. nine μ l of either control oligos, siRNA treatments and miR-506-3p were added to individual Eppendorf tube containing plain media. After a five minute incubation at room temperature, 1.8 μ l of lipofectamine RNAimax was added to the treatment solutions. The tubes were vortexed and then incubated for twenty minutes at room temperature to allow liposome-oligo complexation. After incubation, the working cell suspension was added to the liposome-oligo mixture and placed on the rocker for a minimum of two hours at room temperature. thirty one mL of full culture media was added to a fifty mL tube. The tubes were inverted several times to mix the solution well. ten mL aliquots were plated on 100 mm dishes and placed in the 37 °C incubator for approximately two weeks. Colony formation was observed and then stained using crystal violet stain. The cell media was discarded and Tris buffer was used to wash the cells. After washing the cells, crystal violet stain was added and allowed to sit for approximately twenty minutes at room temperature. After incubation, the crystal violet was discarded and the cells were washed using tap water to remove any remaining excess stain. The plates were left to dry overnight and imaging was performed the following day. Imaging was done with the Canon CanoScan 9000F MarkII scanner for colony counting. Analysis was done using ImageJ.

2.4.3 Forward Transfection for Western Blot

Following cell dissociation, calculations were done to plate 30,000 cells for the control plate and 60,000 cells for the treatment plates. Cells were plated in sixty mm dishes containing full culture media. After twenty four hours, solutions containing the treatments were made. nine μl of control oligo, siRNA treatment or miR-506-3p was added to the Eppendorf tube containing plain culture media. The tubes were then mixed well and incubated at room temperature for five minutes. After incubation, 2.5 μl of Lipofectamine RNAimax liposome was added into each tube and it was vortexed to mix well. The solution mixture was then incubated for twenty minutes at room temperature. During the incubation period, the media from the plates containing the cells were aspirated out. two mL of plain culture media was used to wash the cells and then suctioned off. Five hundred μl of plain culture media was then added to the plates. The liposome-treatment mixtures were then added dropwise to the cells. The mixture was swirled to ensure proper mixing and then placed in the 37 °C incubator for two hours. After this incubation period, two mL of full culture media was added to the dishes and they were placed back into the 37 °C for incubation. After approximately 120 hours, cell lysates were collected.

2.5 Neurite Outgrowth Analysis

Cells were plated and transfected with control oligos, siRNAs targeting the e subunit mRNA or miR-506-3p as described above. Cells were placed in the ZOOM Incucyte Imaging System where cell images were taken at a 20X magnification. Images were taken every twenty four hours for 120 hours. The neurite outgrowth lengths were

calculated using a neurite definition defined for each specific cell line using the NeuroTrack system.

2.6 MTT Assay

After cells were treated and analyzed using the neurite outgrowth assay, the plates were removed from the ZOOM Incucyte Imaging System. fifteen μl of MTT reagent was added to each well and the plates were then placed back into the 37 °C incubator for approximately one hour to allow crystal formation. The plate was then spun down for five minutes and the MTT solution was discarded. fifty μl of DMSO was added to each well to dissolve the crystals and plates were incubated for thirty minutes. The plates were then scanned using a spectrophotometer at both 630 nm and 570 nm. The values associated with 570 nm were subtracted from the values associated with 630 nm to determine the cell viability.

2.7 Western Blot

All western blots followed a general procedure that included cell treatment, cell lysate collection, BCA assay to determine protein concentration, preparation of samples and gels for SDS-PAGE, running of the SDS-PAGE, transferring the protein on the gel to a PVDF membrane, immune-blotting the membranes, and re-blotting the membranes for loading control.

2.7.1 Cell lysate Collection and BCA Assay

Cells were transfected with control oligo, siRNAs targeting the e subunit mRNA or miR-506-3p. After incubation for about 120 hours, the media was discarded and Tris buffer was used to wash the cells four times. The dishes were then patted dry and placed

in the -20°C freezer for three minutes. Plates were then taken out and lysis buffer was added to the plates. The cells were then scraped off and suctioned into an Eppendorf tube. The Eppendorf tubes containing the cells were then placed onto ice and left for ten minutes. After the ten minute incubation, the tubes were spun down at max speed with a microcentrifuge for five minutes. The supernatant was then collected and transferred to a new Eppendorf tube. The BCA assay was performed at this step. In a 96-well plate, a 50:1 ratio of reagent A to B was mixed. Two hundred μl of the A:B solution was added into each well depending on how many samples there were. We had six controls with a known concentration to allow for a comparison with our samples. Five μL of control samples were added to their respective wells followed by 2.5 μL of cell lysate samples. The plate was then incubated for thirty minutes at 37°C. After incubation, plates were read using a spectrophotometer measuring at 562 nm. The protein concentrations were determined using Excel, where the known concentrations were plotted and a best fit trend line was generated to calculate the appropriate concentration for our samples. Typically, fifteen μg of samples was used for each western blot performed. Loading buffer (5X) was added to each sample and they were placed in a heating block for five minutes at 90°C and then stored in the -20°C fridge.

2.7.2 SDS-PAGE

A gel was prepared that typically contained 10% acrylamide. The plates containing the gels were placed in a cassette holder. 1X running buffer (0.25 M Tris, 1.92 M glycine, 1% SDS) was poured inside the cassettes and in the holder. Samples were loaded depending the appropriate amount required to achieve 15 μg . The SDS PAGE was run at 110 volts for 70 minutes to allow the samples to fully resolve via electrophoresis.

2.7.3 Transfer

When SDS-PAGE run time was complete, the gel was removed and placed onto a PVDF membrane that had previously been made hydrophilic using methanol and water soaking. A gel-membrane sandwich was made and placed in a transfer container with an ice pack and run at 150 mA for 90 minutes if only one membrane or 200 mA for 120 minutes if two membranes. The membrane was placed in blocking buffer for overnight incubation

2.7.4 Blotting

The membrane containing the protein samples was taken out of blocking solution and washed four times using TBST wash buffer. The membranes were placed on a parafilm-covered plate and 1000 μ L of primary antibody was added to the membrane and incubated overnight in the 4°C fridge. The primary antibodies used targeted the neural differentiation biomarkers which are rabbit anti-Calnexin, rabbit anti-Beta Tubulin III, rabbit anti-GAP43, and rabbit anti-NSE. After overnight incubation, the membranes were washed again four times with TBST wash buffer and then placed in a secondary antibody solution consisting of 1:10,000 μ L of secondary antibody to wash buffer. The bound primary antibodies were detected using secondary goat anti-rabbit conjugated with horseradish peroxidase (HRP) for 1 hour at room temperature. The membranes were then washed again four times with TBST wash buffer and then placed in a solution of SuperSignal West Pico/Dura Chemiluminescent Substrate for five minutes. The membranes were imaged using ImageLab Software connected to the ChemiDocXRS+ System, and used according to the manual.

2.7.5 Re-blotting

To ensure proper loading, the membranes were washed with TBST wash buffer four times and then placed on a parafilm-covered plate. one mL of primary antibody against calnexin was used to detect our loading control for a one hour incubation. After incubation, the membrane was washed four times and placed in a solution containing a 1:10,000 ratio of secondary to TBST wash buffer and incubated for thirty minutes. After incubation, the membrane was washed four times using TBST wash buffer and placed in a solution of SuperSignal West Pico for five minutes. The membrane was then imaged using ImageLab Software connected to the ChemiDocXRS+ System, and used according to the manual.

2.7.6 Western Blot Quantification

To determine the protein expression levels after treatment of the cell, ImageJ software was used to measure the band density. The software allowed the band densities to be compared to the control sample and took into consideration the loading control via normalization. Excel was used to calculate the appropriate values after ImageJ processed the information.

2.8 Statistical Analysis

2.8.1 Neurite Outgrowth Assay

To determine the effects of the neuroblastoma cells being treated with either control oligos, siRNA against the e subunit mRNA, or miR-506-3p, the neurite lengths were analyzed. A two-tailed t-test was performed to determine the statistical significance between the treatment groups and the control group. Statistical analysis was done using

GraphPad Prism 7, with $P < 0.05$ considering to be statistically significant. GraphPad Prism defined the p-values.

2.8.2 MTT Assay

To determine the effects of the neuroblastoma cells being treated with either control oligos, siRNA against the e subunit mRNA, or miR-506-3p, a two-sample t-test was used via GraphPad Prism 7 to determine the statistical significance between the samples.

2.8.3 Colony Formation Assay

To determine the effects of the neuroblastoma cells being treated with either control oligos, siRNA against the e subunit mRNA, or miR-506-3p, plates were analyzed using ImageJ to determine the relative number of colonies formed after samples treatments. This software is able to estimate the number of colonies and the average colony size. These values were used to perform a two-sample t-test as mentioned before and the statistical significance was determined by comparing the treatment groups against the controls. Statistical analysis was done via GraphPad Prism 7, with a P-Value < 0.05 indicating a statistical significance.

2.9 Neuroblastoma cell lines

The Neuroblastoma cell lines tested were BE(2)-C, SK-N-F1, and SK-N-SH. These cells were obtained from the American Type Culture Collection (ATCC). Kelly

cells were purchased from the cell line repository at the Greehey Children's Cancer Research Institute, University of Texas Health Science Center in San Antonio.

III. RESULTS

3.1 Validation of ATP6V0E1 Knockdown

In order to determine the effect of the ATPase on cell survival, we intended to investigate the effect of depletion of endogenous e subunit levels on neuroblastoma cell survival, proliferation and differentiation. The four molecules that the cells were transfected with are a negative control oligo that is known to not have a gene target, two siRNAs labeled siVATP-1 and siVATP-2 that target distinct regions of the ATP6V0E1 mRNA, and miRNA-506-3p as the positive control (**Figure 5**).

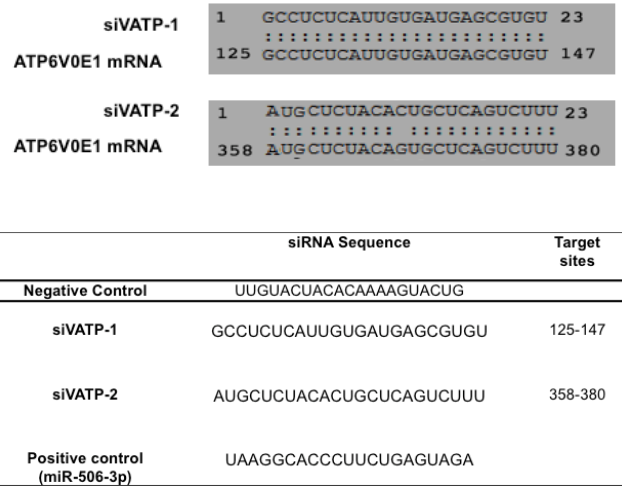


Figure 5. The ribonucleotide sequences of the treatments used. A. Diagram of the corresponding binding site of siVATP-1 at nucleotides 125 to 147 and siVATP-2 binding at region 358 to 380. The nucleotide sequences for the negative control oligo which does not target any gene sequence. siVATP-1 and siVATP-2 sequences targeting distinct regions of the ATP6V0E1 mRNA. The positive control is the previously studied miRNA-506-3p which has been shown to induce neural differentiation and reduce cell viability. <http://workbench.sdsc.edu>

performed on cDNA that was generated from RNA in samples isolated from BE(2)-C neuroblastoma cells harvested seventy two hours following transfection with non-target oligos, siRNAs or miR-506-3p. We determined that ATP6V0E1 mRNA was significantly reduced in ATP6V0E1 siRNA treated samples compared to the non-target control (**Figure 6**). siVATP-2 was able to reduce ATP6V0E1 expression more effectively than siVATP-1. miR-506-3p treated cells significantly reduced ATP6V0E1 mRNA expression

levels compared to the non-target control, in agreement with the gene array data, further validating that the ATP6V0E1 is down regulated by miR-506-3p.

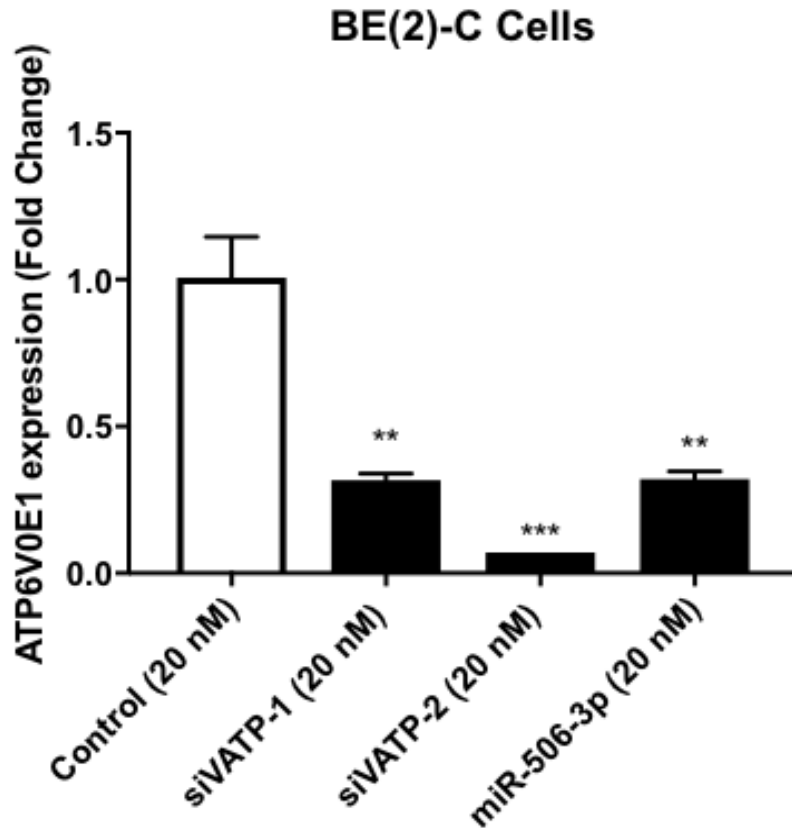


Figure 6. Expression changes of ATP6V0E1 determined by qRT-PCR. BE(2)-C cells were transfected with 20 nM of either negative control oligo, siVATP-1, siVATP-2, or positive control miR-506-2p mimic. qRT-PCR analysis of expression levels are shown **, $p < 0.01$; ***, $p < 0.001$.

3.2 ATP6V0E1 Knockdown Does Not Induce Neuroblastoma Cell Differentiation

Previous studies have shown that miR-506-3p induces neural differentiation in BE(2)-C neuroblastoma cells¹¹. To characterize whether its target gene ATP6V0E1 plays a role in mediating the neural differentiation, BE(2)-C and Kelly neuroblastoma cells' neurite outgrowth was assessed. Knockdown of ATP6V0E1 by both siRNAs did not induce neural outgrowth relative to non-target control treated cells (**Figure 7**). BE(2)-C

cells treated with miR-506-3p displayed an increase in neurite outgrowth relative to the non-target control.

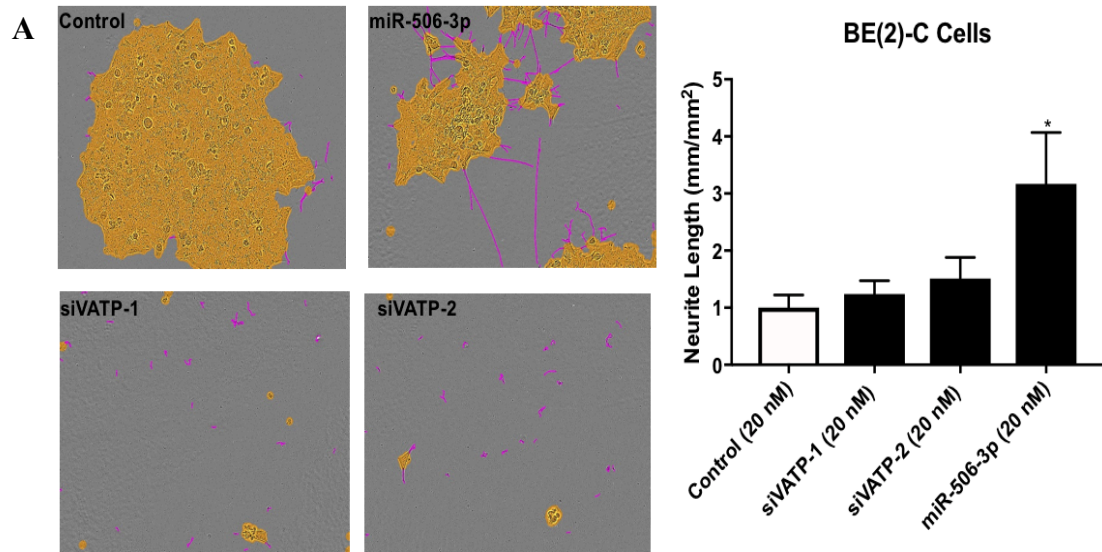


Figure 7: Neurite outgrowth assay on BE(2)-C cells to detect morphological neural differentiation. BE(2)-C cells were transfected with 20 nM of either negative control oligo, siVATP-1, siVATP-2, or positive control miR-506-3p. (A) Representative neurite outgrowth images taken after 120 hours of incubation. The yellow indicates the cell body while the purple identifies the neural outgrowth. (B) Quantification of relative neurite lengths. *, $p < 0.05$

Consistent with the observation that ATP6V0E1 knockdown does not induce neurite outgrowth, there was no increase in neuroblastoma cell differentiation markers, including neuron-specific enolase (NSE), growth-associated protein 43 (GAP43), and β III-Tubulin (Figure 8). GAP43 levels were shown to be similar or slightly below that of the control. miR-506-3p levels of GAP43 were shown to have increased relative to control. β III-Tubulin levels were shown to be similar to that of control, while miR-506-3p shows a greater increase relative to control. NSE protein expression levels after both

siVATP treatments were detected to be higher than both the non-target control and miR-506.

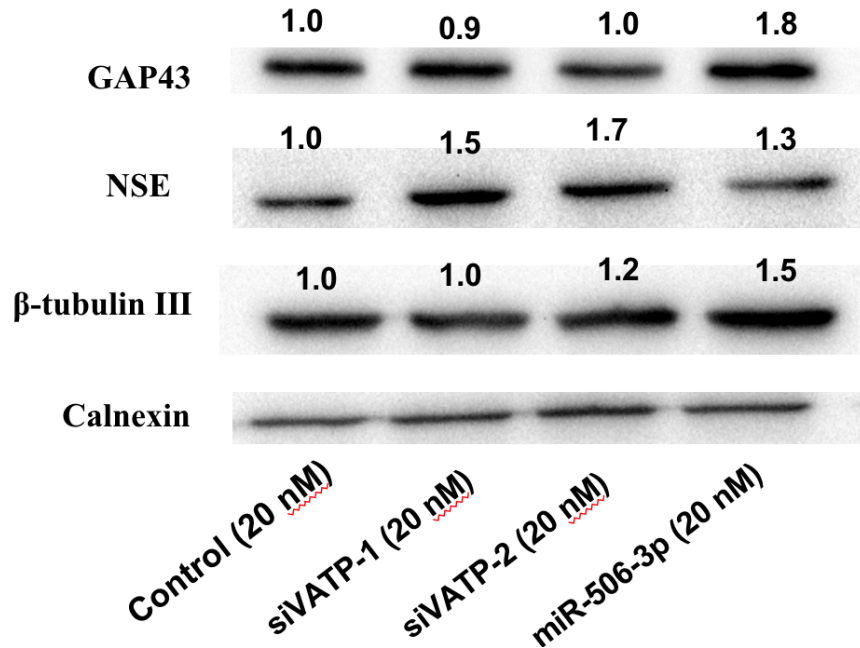


Figure 8: Detection of neural differentiation biomarkers in BE(2)-C cells. Shown are the effects of the corresponding treatments on the expression levels of neuronal biomarkers, with Calnexin protein levels used as a loading control.

Figure 9 shows that the ATP6V0E1 knockdown using both siRNAs did not induce neural outgrowth in Kelly cells, indicating that there was no neural differentiation, which is comparable to that seen in the non-target control treated cells. Kelly cells treated with miR-506-3p displayed an increase in neurite outgrowth relative to the non-target control.

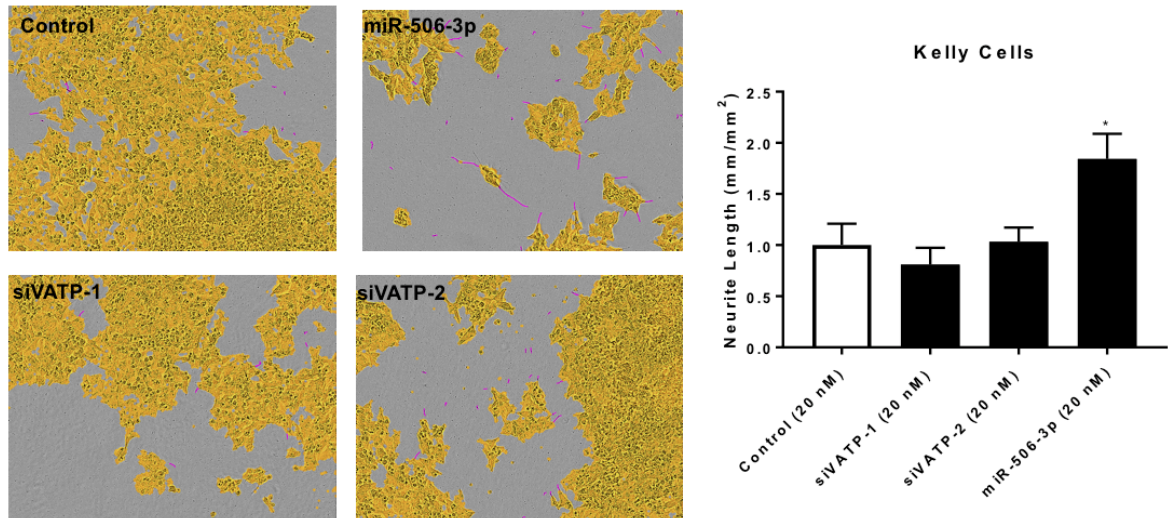


Figure 9: Neurite outgrowth assay on Kelly cells to detect morphological neural differentiation. Kelly cells were transfected with 20 nM of either negative control oligo, siVATP-1, siVATP-2, or positive control miR-506-3p. **(A)** Representative neurite outgrowth images taken after 120 hours of incubation. The yellow indicates the cell body while the purple identifies the neural outgrowth. **(B)** Quantification of relative neurite lengths. *, $p < 0.05$

3.3 Knockdown of *ATP6V0E1* Expression Reduces Cell Viability

To further characterize the role of *ATP6V0E1* in mediating the tumor suppressive effects of miR-506-3p, neuroblastoma cell survival was analyzed using the MTT assays. As shown in **Figure 10**, cell viability was significantly reduced in BE(2)-C neuroblastoma cells after treatment with both siRNAs compared to non-target control. Both of the siRNAs were able to reduce the viability of BE(2)-C neuroblastoma cells to levels observed in miR-506-3p treated cells.

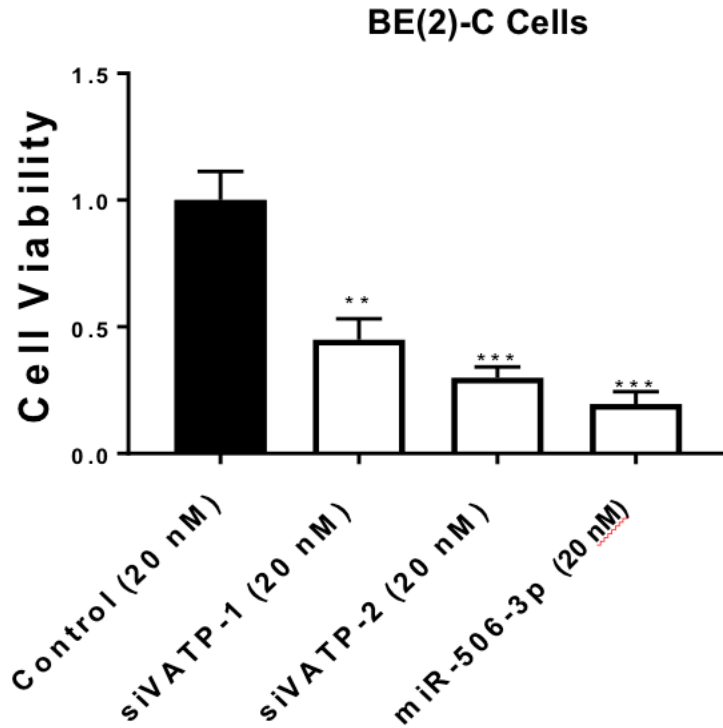


Figure 10: The effect of knockdown of ATP6V0E1 on BE(2)-C cell viability. BE(2)-C cells were transfected with 20 nM of either negative control oligo, siVATP-1, siVATP-2, or positive control miR-506-3p. Statistical analysis of cell viability for control and mimic treatments in BE(2)-C cells. **, $p < 0.01$; ***, $p < 0.001$

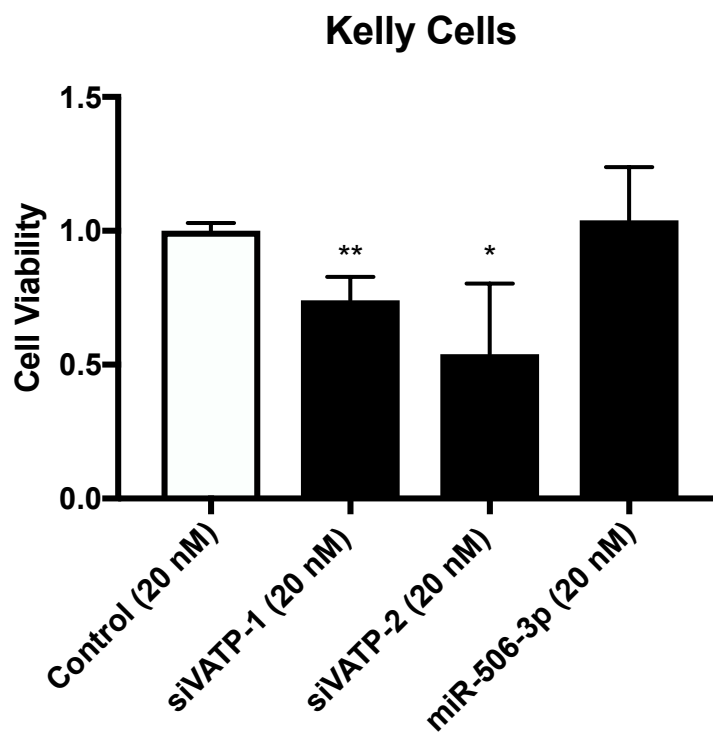


Figure 11: The effect of knockdown of ATP6V0E1 on Kelly cell viability. Kelly cells were transfected with 20 nM of either non-target control oligos, siVATP-1, siVATP-2, or positive control miR-506-3p. Statistical analysis of cell viability for control and mimic treatments in Kelly. *, $p < 0.05$; **, $p < 0.01$

In Kelly cells, cell viability was significantly reduced in Kelly neuroblastoma cells after treatment with both siRNAs compared to non-target control oligos (**figure 11**). miR-506 was not able to reduce cell viability, but in previous studies miR-506 has been shown to be robustly reduce cell viability¹¹.

Figure 12 shows that cell viability was significantly reduced in SKNF1 neuroblastoma cells after treatment with both siRNAs compared to non-target control. Both of the siRNAs were able to reduce cell viability of SKNF1 neuroblastoma cells to levels observed in miR-506-3p treated cells.

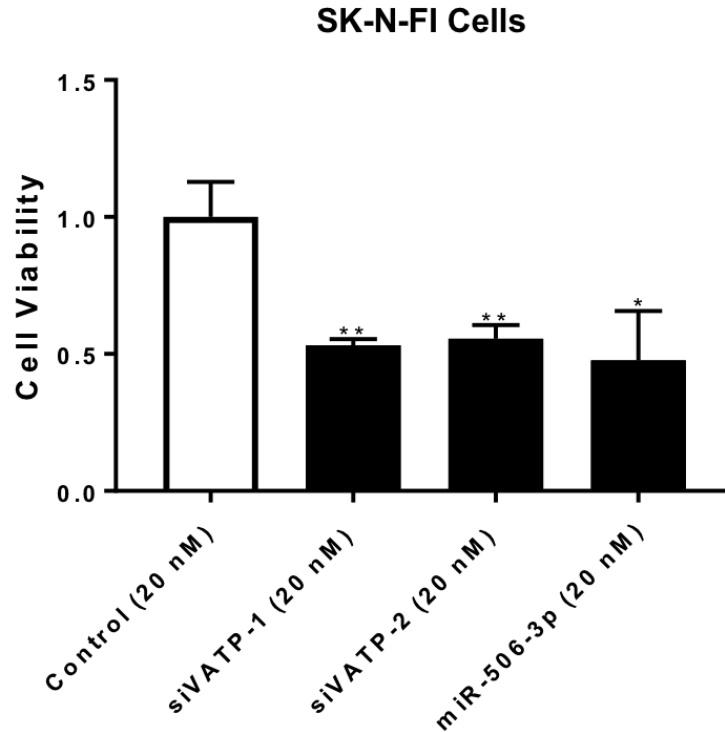


Figure 12: The effect of knockdown of ATP6V0E1 on SK-N-F1 cell viability. SKNF1 cells were transfected with 20 nM of either negative control oligo, siVATP-1, siVATP-2, or positive control miR-506-3p. Statistical analysis of cell viability for control and mimic treatments in SKNF1. *, $p < 0.05$; **, $p < 0.01$; ***, $p < 0.001$; ****, $p < 0.0001$.

Figure 13 shows that cell viability was significantly reduced in HTB-11 neuroblastoma cells after treatment with siVATP-2, but not with siVATP-1. siVATP-2 was able to reduce cell viability of HTB-11 neuroblastoma cells to levels observed in miR-506-3p treated cells. Altogether, these results indicate that the knockdown of ATP6V0E1 expression levels is sufficient to reduce cell viability in various cell lines.

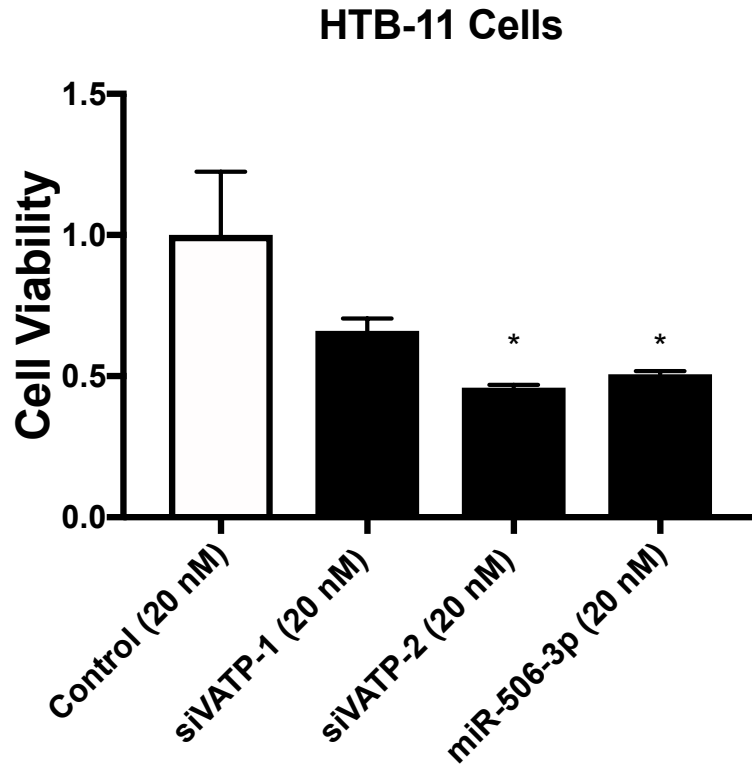


Figure 13: The effect of ATP6V0E1 knockdown on HTB-11 cell viability. HTB-11 cells were transfected with 20 nM of either negative control oligo, siVATP-1, siVATP-2, or positive control miR-506-3p. Statistical analysis of cell viability for control and mimic treatments in BE(2)-C cells. *, $p < 0.05$

3.4 Knockdown of ATP6V0E1 Reduces Cell Proliferation

To determine whether knockdown of ATP6V0E1 expression is sufficient to reduce cellular proliferation, a colony formation assay was performed on both BE(2)-C and Kelly neuroblastoma cells. As seen in **Figure 14**, knockdown of ATP6V0E1 in BE(2)-C neuroblastoma cells was sufficient to reduce colony formation in both siRNA-treated cells compared to the non-target control. Quantitative analysis supported the observations of the reduction in colony formation.

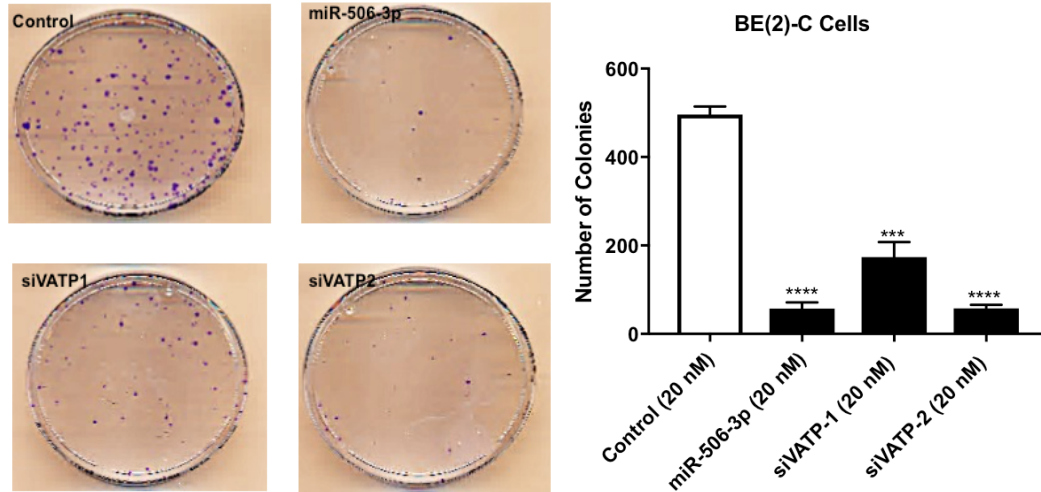


Figure 14: The effect of ATP6V0E1 knockdown on BE(2)-C cell colony formation. BE(2)-C cells were transfected with 20 nM of either negative control oligo, siVATP-1, siVATP-2, or positive control miR-506-3p. (A) Scanned images of the cell plates with their corresponding treatments with cell colonies in purple. Statistical analysis of colony formation is shown in (B). ***, $p < 0.001$; ****, $p < 0.0001$.

As seen in **Figure 15**, knockdown of ATP6V0E1 in Kelly cells was sufficient to reduce colony formation in siVATP-2 treated cells compared to the non-target control but not in siVATP-1 treated cells. SiVATP1 displayed a less effective activity relative to siVATP2, which was able to reduce the number of colonies to a similar level seen with miR-506-3p treat cells. Taken together, these results indicate that the knockdown of ATP6V0E1 expression is sufficient to reduce cellular proliferation.

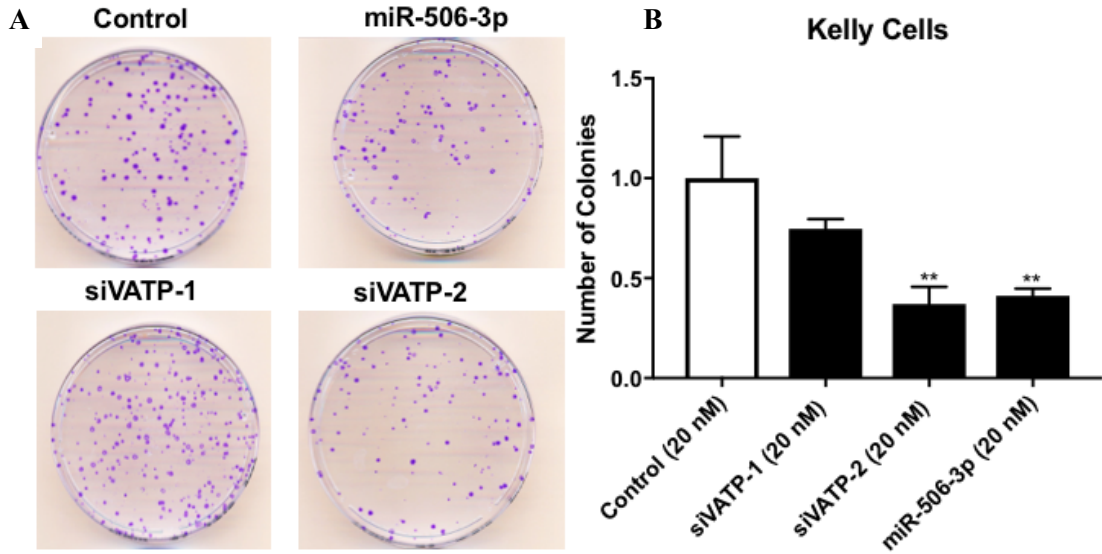


Figure 15: The effect of ATP6V0E1 knockdown on Kelly cell colony formation. Kelly cells were transfected with 20 nM of either negative control oligo, siVATP-1, siVATP-2, or positive control miR-506-3p. **(A)** Scanned images of the plates with their corresponding treatments with colonies in purple. Statistical analysis of colony formation is shown in **(B)**. **, $p < 0.01$

IV. DISCUSSION AND CONCLUSIONS

MiR-506-3p is known to be a potent differentiation inducer and cell growth inhibitor and these effects were confirmed in the current study. As a result, there are potentially two distinct pathways that are being affected via miR-506-3p activity: cell differentiation and cell viability (**Figure 16**). My goal was to determine the role that ATP6V0E1 plays in these processes. Previous reports have shown that the e subunit is essential for the normal function of the V-ATPase.⁶⁹⁻⁷² Our results indicate that knockdown of ATP6V0E1 is sufficient to reduce cell viability and proliferation in BE(2)-C, Kelly, SK-N-F1, and HTB-11 cells. However, knockdown of ATP6V0E1 does not induce neural differentiation in BE(2)-C and Kelly cells. Overall, my study preliminarily characterizes the role of the V-ATPase in mediating the effects of miR-506-3p on neuroblastoma cells. The results suggest that V-ATPase mediated the effect of miR-506-3p on cell survival and proliferation but not the effect on cell differentiation.

Although qRT-PCR analysis of ATP6V0E1 mRNA showed a significant reduction in transcript levels, it would be ideal to determine whether the protein product levels were reduced after ATP6V0E1 knockdown. Our laboratory has tried to detect ATP6V0E1 protein using several commercially available antibodies and to date we have been unable to reliably detect its protein levels, thus limiting our current assessment of ATP6V0E1 knockdown to its mRNA levels.

In our investigation of multiple neuroblastoma cell lines with different genetic backgrounds, we found that the knockdown of ATP6V0E1 was sufficient to reduce cell viability. The observations from the colony formation assays indicated that cellular

proliferation was affected after knockdown of TP6V0E1 expression levels. These results indicate that V-ATPase is essential for neuroblastoma cell survival regardless of the distinct genetic background. It would be interesting to determine whether the knockdown of another V-ATPase subunit or the treatment of a V-ATPase specific inhibitor yields similar results. This would further validate that the V-ATPase is required for neuroblastoma cell survival. Further studies are required to determine whether knockdown of ATP6V0E1 induces cell death or arrests the cells in a non-proliferative quiescent state.

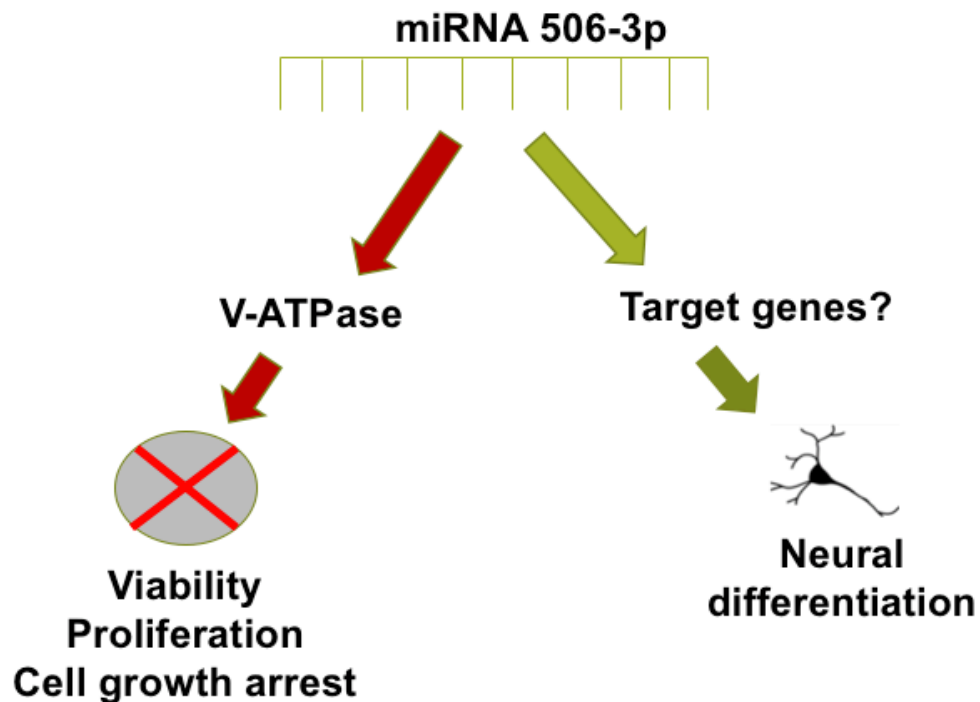


Figure 16: The effects mediated by miR-506-3p. The diagram depicts the two pathways thought to be activated by miR-506-3p. Knockdown of ATP6V0E1 expression is thought to play a significant role in the cell viability pathway. Knockdown has been shown to reduce cell viability and inhibit cell growth.

In conclusion, this data strongly suggests that ATP6V0E1 plays a key role in cell the death pathway mediated by miR-506-3p. The V-ATPase complex has been shown to play key roles in various cellular activities and knockout can be detrimental to cells. Further research is required to fully understand the molecular mechanisms consequences caused by disruption of V-ATPase. The miR-506-3p is known to target many genes as indicated by **Table 2**. Further investigation will allow a better understanding of the fundamental differentiation process and lead to identification of new neural differentiation inducing targets that can be further studied for the development of novel therapies and treatments for neuroblastoma.

In the future, the role of V-ATPase in mediating the tumor suppressive function of miR-506-3p needs to be further characterized by overexpressing ATP6V0E1 in neuroblastoma cells. Transfection of the neuroblastoma cells using the appropriate vector will overexpress the ATP6V0E1 protein. The expression vector will not contain a 3'UTR, allowing 100% overexpression without the interference of miR-506-3p. In addition, a vector can be made where ATP6V0E1 will be overexpressed but with the addition of its 3'UTR to allow endogenous miR-506 to interfere. This will allow us to analyze the effects that the V-ATPase and miR-506 have on each other.

The mechanism involved in the reduction of cell viability and proliferation still need to be further investigated. Western blot analysis can allow us to determine the pathways underlying the reduction of cell viability and proliferation. In addition additional subunits of the V-ATPase can be knocked down to determine if these same effects are observed. V-ATPase specific inhibitors would further validate our

observations and would strengthen the idea that V-ATPase plays a role in neuroblastoma cell survival and proliferation.

REFERENCES

1. Ries LA, S. M., Gurney JG, Linet M, Tamra T, Young JL, Bunin GR (eds), Cancer Incidence and Survival among Children and Adolescents: United States SEER Program 1975-1995. *National Cancer Institute, SEER Program. NIH Pub. No. 99-4649. Bethesda, MD, 1999. 1999.*
2. Mosse, Y. P.; Deyell, R. J.; Berthold, F.; Nagakawara, A.; Ambros, P. F.; Monclair, T.; Cohn, S. L.; Pearson, A. D.; London, W. B.; Matthay, K. K., Neuroblastoma in older children, adolescents and young adults: a report from the International Neuroblastoma Risk Group project. *Pediatr Blood Cancer* **2014**, *61* (4), 627-35.
3. Board, C. N. E., Neuroblastoma - Childhood - Statistics. *American Society of Clinical Oncology (ASCO) - Cancer.Net* **Jun 25, 2012.**
4. Louis, C. U.; Shohet, J. M., Neuroblastoma: molecular pathogenesis and therapy. *Annu Rev Med* **2015**, *66*, 49-63.
5. Adams, G. A.; Shochat, S. J.; Smith, E. I.; Shuster, J. J.; Joshi, V. V.; Altshuler, G.; Hayes, F. A.; Nitschke, R.; McWilliams, N.; Castleberry, R. P., Thoracic neuroblastoma: a Pediatric Oncology Group study. *J Pediatr Surg* **1993**, *28* (3), 372-7; discussion 377-8.
6. Huber, K., The sympathoadrenal cell lineage: specification, diversification, and new perspectives. *Dev Biol* **2006**, *298* (2), 335-43.
7. De Zio, D.; Giunta, L.; Corvaro, M.; Ferraro, E.; Cecconi, F., Expanding roles of programmed cell death in mammalian neurodevelopment. *Semin Cell Dev Biol* **2005**, *16* (2), 281-94.
8. Maris, J. M.; Hogarty, M. D.; Bagatell, R.; Cohn, S. L., Neuroblastoma. *Lancet* **2007**, *369* (9579), 2106-20.
9. Park, J. R.; Bagatell, R.; London, W. B.; Maris, J. M.; Cohn, S. L.; Mattay, K. K.; Hogarty, M.; Committee, C. O. G. N., Children's Oncology Group's 2013 blueprint for research: neuroblastoma. *Pediatr Blood Cancer* **2013**, *60* (6), 985-93.
10. Meany, H. J.; London, W. B.; Ambros, P. F.; Matthay, K. K.; Monclair, T.; Simon, T.; Garaventa, A.; Berthold, F.; Nakagawara, A.; Cohn, S. L.; Pearson, A. D.; Park, J. R., Significance of clinical and biologic features in Stage 3 neuroblastoma: a report from the International Neuroblastoma Risk Group project. *Pediatr Blood Cancer* **2014**, *61* (11), 1932-9.

11. Zhao, Z.; Ma, X.; Hsiao, T. H.; Lin, G.; Kostı, A.; Yu, X.; Suresh, U.; Chen, Y.; Tomlinson, G. E.; Pertsemlidis, A.; Du, L., A high-content morphological screen identifies novel microRNAs that regulate neuroblastoma cell differentiation. *Oncotarget* **2014**, *5* (9), 2499-512.
12. Cruz, F. D.; Matushansky, I., Solid tumor differentiation therapy - is it possible? *Oncotarget* **2012**, *3* (5), 559-67.
13. Park, J. R.; Eggert, A.; Caron, H., Neuroblastoma: biology, prognosis, and treatment. *Hematol Oncol Clin North Am* **2010**, *24* (1), 65-86.
14. Matthay, K. K.; Villablanca, J. G.; Seeger, R. C.; Stram, D. O.; Harris, R. E.; Ramsay, N. K.; Swift, P.; Shimada, H.; Black, C. T.; Brodeur, G. M.; Gerbing, R. B.; Reynolds, C. P., Treatment of high-risk neuroblastoma with intensive chemotherapy, radiotherapy, autologous bone marrow transplantation, and 13-cis-retinoic acid. Children's Cancer Group. *N Engl J Med* **1999**, *341* (16), 1165-73.
15. Matthay, K. K.; Reynolds, C. P.; Seeger, R. C.; Shimada, H.; Adkins, E. S.; Haas-Kogan, D.; Gerbing, R. B.; London, W. B.; Villablanca, J. G., Long-term results for children with high-risk neuroblastoma treated on a randomized trial of myeloablative therapy followed by 13-cis-retinoic acid: a children's oncology group study. *J Clin Oncol* **2009**, *27* (7), 1007-13.
16. Sidell, N.; Altman, A.; Haussler, M. R.; Seeger, R. C., Effects of retinoic acid (RA) on the growth and phenotypic expression of several human neuroblastoma cell lines. *Exp Cell Res* **1983**, *148* (1), 21-30.
17. Reynolds, C. P.; Matthay, K. K.; Villablanca, J. G.; Maurer, B. J., Retinoid therapy of high-risk neuroblastoma. *Cancer Lett* **2003**, *197* (1-2), 185-92.
18. Zhao, Z.; Ma, X.; Sung, D.; Li, M.; Kostı, A.; Lin, G.; Chen, Y.; Pertsemlidis, A.; Hsiao, T. H.; Du, L., microRNA-449a functions as a tumor suppressor in neuroblastoma through inducing cell differentiation and cell cycle arrest. *RNA Biol* **2015**, *12* (5), 538-54.
19. Cai, Y.; Yu, X.; Hu, S.; Yu, J., A brief review on the mechanisms of miRNA regulation. *Genomics Proteomics Bioinformatics* **2009**, *7* (4), 147-54.
20. Denzler, R.; McGeary, S. E.; Title, A. C.; Agarwal, V.; Bartel, D. P.; Stoffel, M., Impact of MicroRNA Levels, Target-Site Complementarity, and Cooperativity on Competing Endogenous RNA-Regulated Gene Expression. *Mol Cell* **2016**, *64* (3), 565-579.
21. Grimson, A.; Farh, K. K.; Johnston, W. K.; Garrett-Engele, P.; Lim, L. P.; Bartel, D. P., MicroRNA targeting specificity in mammals: determinants beyond seed pairing. *Mol Cell* **2007**, *27* (1), 91-105.
22. Friedman, R. C.; Farh, K. K.; Burge, C. B.; Bartel, D. P., Most mammalian mRNAs are conserved targets of microRNAs. *Genome Res* **2009**, *19* (1), 92-105.

23. Li, M.; Li, J.; Ding, X.; He, M.; Cheng, S. Y., microRNA and cancer. *AAPS J* **2010**, *12* (3), 309-17.
24. Volinia, S.; Calin, G. A.; Liu, C. G.; Ambs, S.; Cimmino, A.; Petrocca, F.; Visone, R.; Iorio, M.; Roldo, C.; Ferracin, M.; Prueitt, R. L.; Yanaihara, N.; Lanza, G.; Scarpa, A.; Vecchione, A.; Negrini, M.; Harris, C. C.; Croce, C. M., A microRNA expression signature of human solid tumors defines cancer gene targets. *Proc Natl Acad Sci U S A* **2006**, *103* (7), 2257-61.
25. Smirnova, L.; Grafe, A.; Seiler, A.; Schumacher, S.; Nitsch, R.; Wulczyn, F. G., Regulation of miRNA expression during neural cell specification. *Eur J Neurosci* **2005**, *21* (6), 1469-77.
26. Calin, G. A.; Dumitru, C. D.; Shimizu, M.; Bichi, R.; Zupo, S.; Noch, E.; Aldler, H.; Rattan, S.; Keating, M.; Rai, K.; Rassenti, L.; Kipps, T.; Negrini, M.; Bullrich, F.; Croce, C. M., Frequent deletions and down-regulation of micro- RNA genes miR15 and miR16 at 13q14 in chronic lymphocytic leukemia. *Proc Natl Acad Sci U S A* **2002**, *99* (24), 15524-9.
27. Garzon, R.; Pichiorri, F.; Palumbo, T.; Visentini, M.; Aqeilan, R.; Cimmino, A.; Wang, H.; Sun, H.; Volinia, S.; Alder, H.; Calin, G. A.; Liu, C. G.; Andreeff, M.; Croce, C. M., MicroRNA gene expression during retinoic acid-induced differentiation of human acute promyelocytic leukemia. *Oncogene* **2007**, *26* (28), 4148-57.
28. Pasquinelli, A. E.; Reinhart, B. J.; Slack, F.; Martindale, M. Q.; Kuroda, M. I.; Maller, B.; Hayward, D. C.; Ball, E. E.; Degnan, B.; Muller, P.; Spring, J.; Srinivasan, A.; Fishman, M.; Finnerty, J.; Corbo, J.; Levine, M.; Leahy, P.; Davidson, E.; Ruvkun, G., Conservation of the sequence and temporal expression of let-7 heterochronic regulatory RNA. *Nature* **2000**, *408* (6808), 86-9.
29. Yanaihara, N.; Caplen, N.; Bowman, E.; Seike, M.; Kumamoto, K.; Yi, M.; Stephens, R. M.; Okamoto, A.; Yokota, J.; Tanaka, T.; Calin, G. A.; Liu, C. G.; Croce, C. M.; Harris, C. C., Unique microRNA molecular profiles in lung cancer diagnosis and prognosis. *Cancer Cell* **2006**, *9* (3), 189-98.
30. Takamizawa, J.; Konishi, H.; Yanagisawa, K.; Tomida, S.; Osada, H.; Endoh, H.; Harano, T.; Yatabe, Y.; Nagino, M.; Nimura, Y.; Mitsudomi, T.; Takahashi, T., Reduced expression of the let-7 microRNAs in human lung cancers in association with shortened postoperative survival. *Cancer Res* **2004**, *64* (11), 3753-6.
31. Senior, A. E.; Nadanaciva, S.; Weber, J., The molecular mechanism of ATP synthesis by F1F0-ATP synthase. *Biochim Biophys Acta* **2002**, *1553* (3), 188-211.
32. Bickel-Sandkottter, S.; Gartner, W.; Dane, M., Conversion of energy in halobacteria: ATP synthesis and phototaxis. *Arch Microbiol* **1996**, *166* (1), 1-11.
33. Lutsenko, S.; Kaplan, J. H., Organization of P-type ATPases: significance of structural diversity. *Biochemistry* **1995**, *34* (48), 15607-13.

34. Kuhlbrandt, W., Biology, structure and mechanism of P-type ATPases. *Nat Rev Mol Cell Biol* **2004**, *5* (4), 282-95.
35. Plesner, L., Ecto-ATPases: identities and functions. *Int Rev Cytol* **1995**, *158*, 141-214.
36. Muench, S. P.; Trinick, J.; Harrison, M. A., Structural divergence of the rotary ATPases. *Q Rev Biophys* **2011**, *44* (3), 311-56.
37. Ohsumi, Y.; Anraku, Y., Active transport of basic amino acids driven by a proton motive force in vacuolar membrane vesicles of *Saccharomyces cerevisiae*. *J Biol Chem* **1981**, *256* (5), 2079-82.
38. Stransky, L.; Cotter, K.; Forgacs, M., The Function of V-ATPases in Cancer. *Physiol Rev* **2016**, *96* (3), 1071-91.
39. Sun-Wada, G. H.; Wada, Y.; Futai, M., Diverse and essential roles of mammalian vacuolar-type proton pump ATPase: toward the physiological understanding of inside acidic compartments. *Biochim Biophys Acta* **2004**, *1658* (1-2), 106-14.
40. Yoshimori, T.; Yamamoto, A.; Moriyama, Y.; Futai, M.; Tashiro, Y., Bafilomycin A1, a specific inhibitor of vacuolar-type H(+)-ATPase, inhibits acidification and protein degradation in lysosomes of cultured cells. *J Biol Chem* **1991**, *266* (26), 17707-12.
41. Pisoni, R. L.; Thoene, J. G.; Christensen, H. N., Detection and characterization of carrier-mediated cationic amino acid transport in lysosomes of normal and cystinotic human fibroblasts. Role in therapeutic cystine removal? *J Biol Chem* **1985**, *260* (8), 4791-8.
42. Zoncu, R.; Bar-Peled, L.; Efeyan, A.; Wang, S.; Sancak, Y.; Sabatini, D. M., mTORC1 senses lysosomal amino acids through an inside-out mechanism that requires the vacuolar H(+)-ATPase. *Science* **2011**, *334* (6056), 678-83.
43. Moriyama, Y.; Maeda, M.; Futai, M., The role of V-ATPase in neuronal and endocrine systems. *J Exp Biol* **1992**, *172*, 171-8.
44. Wagner, C. A.; Finberg, K. E.; Breton, S.; Marshansky, V.; Brown, D.; Geibel, J. P., Renal vacuolar H⁺-ATPase. *Physiol Rev* **2004**, *84* (4), 1263-314.
45. Qin, A.; Cheng, T. S.; Pavlos, N. J.; Lin, Z.; Dai, K. R.; Zheng, M. H., V-ATPases in osteoclasts: structure, function and potential inhibitors of bone resorption. *Int J Biochem Cell Biol* **2012**, *44* (9), 1422-35.
46. Huss, M.; Wiczorek, H., Inhibitors of V-ATPases: old and new players. *J Exp Biol* **2009**, *212* (Pt 3), 341-6.

47. Huss, M.; Ingenhorst, G.; Konig, S.; Gassel, M.; Drose, S.; Zeeck, A.; Altendorf, K.; Wiczorek, H., Concanamycin A, the specific inhibitor of V-ATPases, binds to the V(o) subunit c. *J Biol Chem* **2002**, *277* (43), 40544-8.
48. Wang, Y.; Inoue, T.; Forgac, M., Subunit a of the yeast V-ATPase participates in binding of bafilomycin. *J Biol Chem* **2005**, *280* (49), 40481-8.
49. Sasse, F.; Steinmetz, H.; Hofle, G.; Reichenbach, H., Archazolids, new cytotoxic macrolactones from *Archangium gephyra* (Myxobacteria). Production, isolation, physico-chemical and biological properties. *J Antibiot (Tokyo)* **2003**, *56* (6), 520-5.
50. Huss, M.; Sasse, F.; Kunze, B.; Jansen, R.; Steinmetz, H.; Ingenhorst, G.; Zeeck, A.; Wiczorek, H., Archazolid and apicularen: novel specific V-ATPase inhibitors. *BMC Biochem* **2005**, *6*, 13.
51. Forgac, M., Vacuolar ATPases: rotary proton pumps in physiology and pathophysiology. *Nat Rev Mol Cell Biol* **2007**, *8* (11), 917-29.
52. Wu, Y. C.; Wu, W. K.; Li, Y.; Yu, L.; Li, Z. J.; Wong, C. C.; Li, H. T.; Sung, J. J.; Cho, C. H., Inhibition of macroautophagy by bafilomycin A1 lowers proliferation and induces apoptosis in colon cancer cells. *Biochem Biophys Res Commun* **2009**, *382* (2), 451-6.
53. Nakashima, S.; Hiraku, Y.; Tada-Oikawa, S.; Hishita, T.; Gabazza, E. C.; Tamaki, S.; Imoto, I.; Adachi, Y.; Kawanishi, S., Vacuolar H⁺-ATPase inhibitor induces apoptosis via lysosomal dysfunction in the human gastric cancer cell line MKN-1. *J Biochem* **2003**, *134* (3), 359-64.
54. von Schwarzenberg, K.; Wiedmann, R. M.; Oak, P.; Schulz, S.; Zischka, H.; Wanner, G.; Efferth, T.; Trauner, D.; Vollmar, A. M., Mode of cell death induction by pharmacological vacuolar H⁺-ATPase (V-ATPase) inhibition. *J Biol Chem* **2013**, *288* (2), 1385-96.
55. Eyraud, V.; Balmand, S.; Karaki, L.; Rahioui, I.; Sivignon, C.; Delmas, A. F.; Royer, C.; Rahbe, Y.; Da Silva, P.; Gressent, F., The interaction of the bioinsecticide PA1b (Pea Albumin 1 subunit b) with the insect V-ATPase triggers apoptosis. *Sci Rep* **2017**, *7* (1), 4902.
56. Kim, H.; Kim, A.; Cunningham, K. W., Vacuolar H⁺-ATPase (V-ATPase) promotes vacuolar membrane permeabilization and nonapoptotic death in stressed yeast. *J Biol Chem* **2012**, *287* (23), 19029-39.
57. Syntichaki, P.; Samara, C.; Tavernarakis, N., The vacuolar H⁺ -ATPase mediates intracellular acidification required for neurodegeneration in *C. elegans*. *Curr Biol* **2005**, *15* (13), 1249-54.
58. Cross, R. L., The rotary binding change mechanism of ATP synthases. *Biochim Biophys Acta* **2000**, *1458* (2-3), 270-5.

59. Ihara, K.; Abe, T.; Sugimura, K. I.; Mukohata, Y., HALOBACTERIAL A-ATP SYNTHASE IN RELATION TO V-ATPase. *J Exp Biol* **1992**, *172* (Pt 1), 475-485.
60. Preston, R. A.; Murphy, R. F.; Jones, E. W., Assay of vacuolar pH in yeast and identification of acidification-defective mutants. *Proc Natl Acad Sci U S A* **1989**, *86* (18), 7027-31.
61. Tomashek, J. J.; Sonnenburg, J. L.; Artimovich, J. M.; Klionsky, D. J., Resolution of subunit interactions and cytoplasmic subcomplexes of the yeast vacuolar proton-translocating ATPase. *J Biol Chem* **1996**, *271* (17), 10397-404.
62. Yamagata, S. K.; Parsons, S. M., Cholinergic synaptic vesicles contain a V-type and a P-type ATPase. *J Neurochem* **1989**, *53* (5), 1354-62.
63. Liu, Y.; Edwards, R. H., The role of vesicular transport proteins in synaptic transmission and neural degeneration. *Annu Rev Neurosci* **1997**, *20*, 125-56.
64. Maycox, P. R.; Hell, J. W.; Jahn, R., Amino acid neurotransmission: spotlight on synaptic vesicles. *Trends Neurosci* **1990**, *13* (3), 83-7.
65. Vavassori, S.; Mayer, A., A new life for an old pump: V-ATPase and neurotransmitter release. *J Cell Biol* **2014**, *205* (1), 7-9.
66. Puopolo, K.; Forgacs, M., Functional reassembly of the coated vesicle proton pump. *J Biol Chem* **1990**, *265* (25), 14836-41.
67. Kane, P. M.; Tarsio, M.; Liu, J., Early steps in assembly of the yeast vacuolar H⁺-ATPase. *J Biol Chem* **1999**, *274* (24), 17275-83.
68. Marshansky, V.; Rubinstein, J. L.; Gruber, G., Eukaryotic V-ATPase: novel structural findings and functional insights. *Biochim Biophys Acta* **2014**, *1837* (6), 857-79.
69. Ludwig, J.; Kerscher, S.; Brandt, U.; Pfeiffer, K.; Getlawi, F.; Apps, D. K.; Schagger, H., Identification and characterization of a novel 9.2-kDa membrane sector-associated protein of vacuolar proton-ATPase from chromaffin granules. *J Biol Chem* **1998**, *273* (18), 10939-47.
70. Rawson, S.; Harrison, M. A.; Muench, S. P., Rotating with the brakes on and other unresolved features of the vacuolar ATPase. *Biochem Soc Trans* **2016**, *44* (3), 851-5.
71. Sambade, M.; Kane, P. M., The yeast vacuolar proton-translocating ATPase contains a subunit homologous to the *Manduca sexta* and bovine e subunits that is essential for function. *J Biol Chem* **2004**, *279* (17), 17361-5.
72. Compton, M. A.; Graham, L. A.; Stevens, T. H., Vma9p (subunit e) is an integral membrane V₀ subunit of the yeast V-ATPase. *J Biol Chem* **2006**, *281* (22), 15312-9.

73. Blake-Palmer, K. G.; Su, Y.; Smith, A. N.; Karet, F. E., Molecular cloning and characterization of a novel form of the human vacuolar H⁺-ATPase e-subunit: an essential proton pump component. *Gene* **2007**, *393* (1-2), 94-100.
74. Bueler, S. A.; Rubinstein, J. L., Vma9p need not be associated with the yeast V-ATPase for fully-coupled proton pumping activity in vitro. *Biochemistry* **2015**, *54* (3), 853-8.
75. Merzendorfer, H.; Huss, M.; Schmid, R.; Harvey, W. R.; Wiczorek, H., A novel insect V-ATPase subunit M9.7 is glycosylated extensively. *J Biol Chem* **1999**, *274* (24), 17372-8.
76. Rawson, S.; Phillips, C.; Huss, M.; Tiburcy, F.; Wiczorek, H.; Trinick, J.; Harrison, M. A.; Muench, S. P., Structure of the vacuolar H⁺-ATPase rotary motor reveals new mechanistic insights. *Structure* **2015**, *23* (3), 461-71.
77. Muench, S. P.; Rawson, S.; Eyraud, V.; Delmas, A. F.; Da Silva, P.; Phillips, C.; Trinick, J.; Harrison, M. A.; Gressent, F.; Huss, M., PA1b inhibitor binding to subunits c and e of the vacuolar ATPase reveals its insecticidal mechanism. *J Biol Chem* **2014**, *289* (23), 16399-408.
78. Karet, F. E.; Finberg, K. E.; Nelson, R. D.; Nayir, A.; Mocan, H.; Sanjad, S. A.; Rodriguez-Soriano, J.; Santos, F.; Cremers, C. W.; Di Pietro, A.; Hoffbrand, B. I.; Winiarski, J.; Bakkaloglu, A.; Ozen, S.; Dusunsel, R.; Goodyer, P.; Hulton, S. A.; Wu, D. K.; Skvorak, A. B.; Morton, C. C.; Cunningham, M. J.; Jha, V.; Lifton, R. P., Mutations in the gene encoding B1 subunit of H⁺-ATPase cause renal tubular acidosis with sensorineural deafness. *Nat Genet* **1999**, *21* (1), 84-90.
79. Frattini, A.; Orchard, P. J.; Sobacchi, C.; Giliani, S.; Abinun, M.; Mattsson, J. P.; Keeling, D. J.; Andersson, A. K.; Wallbrandt, P.; Zecca, L.; Notarangelo, L. D.; Vezzoni, P.; Villa, A., Defects in TCIRG1 subunit of the vacuolar proton pump are responsible for a subset of human autosomal recessive osteopetrosis. *Nat Genet* **2000**, *25* (3), 343-6.
80. Li, Y. P.; Chen, W.; Liang, Y.; Li, E.; Stashenko, P., Atp6i-deficient mice exhibit severe osteopetrosis due to loss of osteoclast-mediated extracellular acidification. *Nat Genet* **1999**, *23* (4), 447-51.
81. Gillies, R. J.; Robey, I.; Gatenby, R. A., Causes and consequences of increased glucose metabolism of cancers. *J Nucl Med* **2008**, *49 Suppl 2*, 24S-42S.
82. Racker, E., Bioenergetics and the problem of tumor growth. *Am Sci* **1972**, *60* (1), 56-63.
83. Sennoune, S. R.; Bakunts, K.; Martinez, G. M.; Chua-Tuan, J. L.; Kebir, Y.; Attaya, M. N.; Martinez-Zaguilan, R., Vacuolar H⁺-ATPase in human breast cancer cells with distinct metastatic potential: distribution and functional activity. *Am J Physiol Cell Physiol* **2004**, *286* (6), C1443-52.

84. Ohta, T.; Numata, M.; Yagishita, H.; Futagami, F.; Tsukioka, Y.; Kitagawa, H.; Kayahara, M.; Nagakawa, T.; Miyazaki, I.; Yamamoto, M.; Iseki, S.; Ohkuma, S., Expression of 16 kDa proteolipid of vacuolar-type H(+)-ATPase in human pancreatic cancer. *Br J Cancer* **1996**, *73* (12), 1511-7.
85. Gottlieb, R. A.; Giesing, H. A.; Zhu, J. Y.; Engler, R. L.; Babior, B. M., Cell acidification in apoptosis: granulocyte colony-stimulating factor delays programmed cell death in neutrophils by up-regulating the vacuolar H(+)-ATPase. *Proc Natl Acad Sci U S A* **1995**, *92* (13), 5965-8.
86. Hashimoto, S.; Ishisaki, A.; Yamato, K.; Aiko, K.; Amagasa, T.; Nishihara, T., Intracellular apoptosis-inducing factor is induced by a vacuolar type H⁺-ATPase inhibitor in B lineage cells. *J Cell Physiol* **2001**, *186* (1), 65-72.